P2

MARTIAN SURFACE COORDINATES

SPONSORED BY THE JET PROPULSION LABORATORY, CALIFORNIA INSTITUTE OF TECHNOLOGY

DRA

MERTON E. DAVIES
DAVID W. G. ARTHUR

R-1252-JPL
APRIL 1973

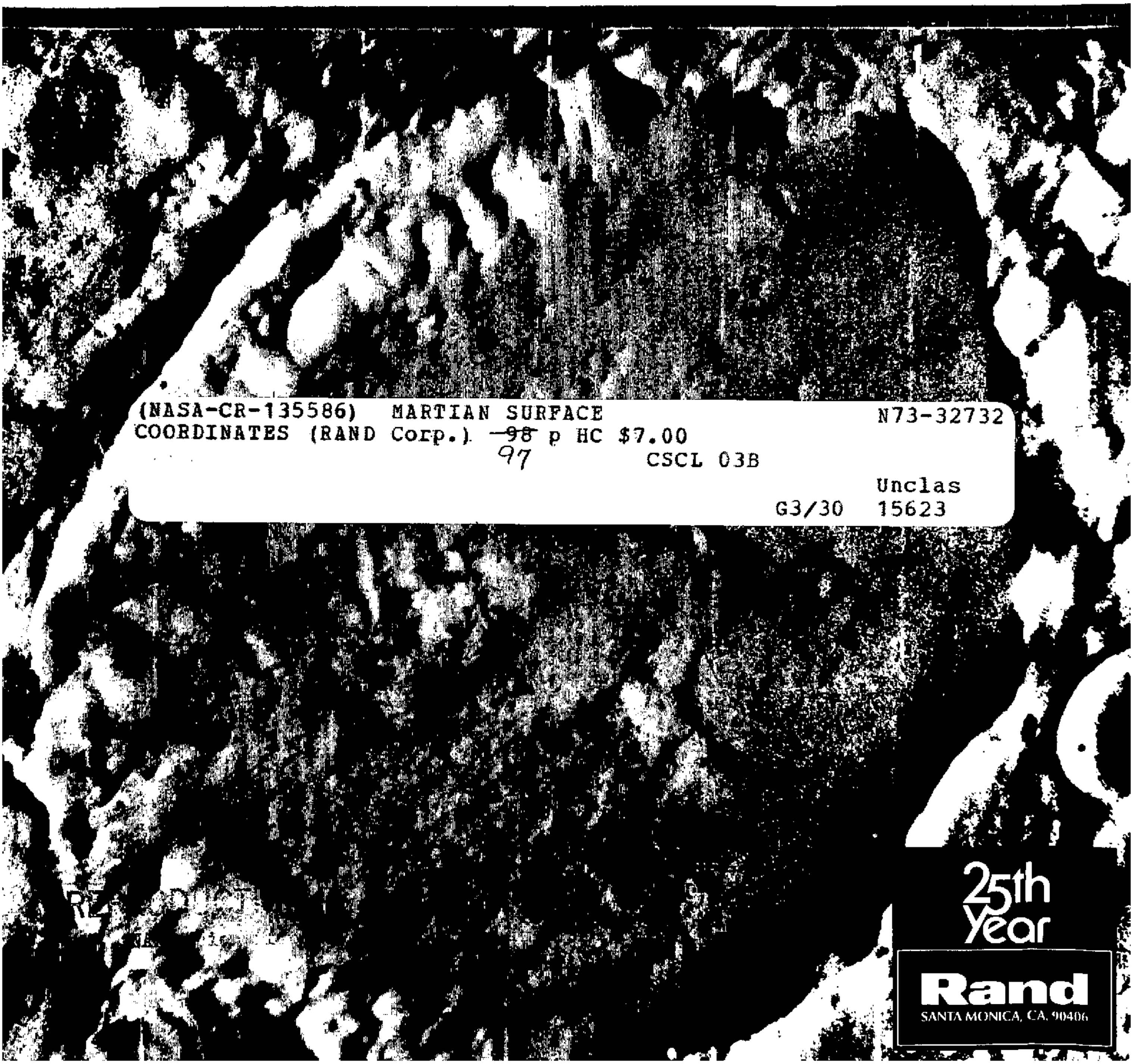

(NASA-CR-135586) MARTIAN SURFACE COORDINATES (RAND Corp.) ~~98~~ 97 p HC $7.00 CSCL 03B
N73-32732
Unclas
G3/30 15623

This research was supported by the Jet Propulsion Laboratory, California Institute of Technology, through Rand Contract No. 953011 and WO-8122 with the U. S. Geological Survey. Reports of the Rand Corporation do not necessarily reflect the opinions or policies of the sponsors of Rand research.

Published by The Rand Corporation

MARTIAN SURFACE COORDINATES

SPONSORED BY THE JET PROPULSION LABORATORY,
CALIFORNIA INSTITUTE OF TECHNOLOGY

MERTON E. DAVIES
DAVID W. G. ARTHUR

R-1252-JPL
APRIL 1973

Rand
SANTA MONICA, CA. 90406

PREFACE

This report is one of a series of papers prepared for publication in the July 1973 issue of the *Journal of Geophysical Research* by members of the Mariner 9 science experimenter teams. Previous reports of the experimenter teams were published in *Science*, 21 January 1972 and in *Icarus*, Vol. 17, No. 2, October 1972, and Vol. 18, No. 1, January 1973.

Merton E. Davies is a member of the senior staff of The Rand Corporation, Santa Monica, California, and David G. W. Arthur is a member of the staff of the Astrogeology Branch of the United States Geological Survey, Flagstaff, Arizona.

CONTENTS

PRECEDING PAGE BLANK NOT FILMED

TABLES

Page intentionally left blank

[redacted]

FIGURES

[redacted]

ABSTRACT

This paper presents methods and results for primary and secondary triangulation of the martian surface. The primary network is based on multiphotograph stereophotogrammetry in which the pictures are rotated around fixed centers; these centers are provided as spacecraft stations from the tracking data. The computations use the latest Mars spin axis determined by Mariner 9 experiments and the new first meridian passing through a small crater, Airy-0, seen on Mariner 9 imagery. The secondary triangulation is performed in the map plane using rectified pictures as map fragments, assumed to be of correct shape. 1205 primary positions are given in this paper.

I. INTRODUCTION

Astronomers have long studied the surface markings of Mars and have used them to establish coordinate systems of the planet's surface. A comprehensive effort to combine the results of all of the telescopic observations into a single network of positions has recently been completed by de Vaucouleurs [1965, 1969]. In contrast to the classical nets that were based on albedo markings, the Mariner 6 and 7 flyby missions offered the first opportunity to establish a control net based on surface topography. This work was reported by Davies and Berg [1970] and Davies [1971]. Only 21 of the near-encounter pictures of Mars were in the resolution regime best suited for the identification and measurement of control points. These few pictures covered a very small area, so low-resolution, far-encounter pictures were used to build the control net over most of the martian surface.

The resolution of the pictures from the Mariner 9 mission determines the distribution of the control points on Mars, as well as the gaps in the planet-wide control net. Work on this net began early in 1972 and the net has continued to expand since that time. Progress was first reported in August 1972 [Davies, 1972] and was updated in November 1972.

The Mariner 9 orbit had a period of about 11.97 hours, an inclination of 65°, and a periapsis altitude of 1387 km, which was raised to 1650 km during a trim maneuver on December 30, 1971. Periapsis occurred at a latitude of about 23° south and varied slightly during the life of the mission. Thus, high-resolution pictures (the mapping sequences) were taken from a distance of less than 2000 km from about 65° south to 15° north and from about 3500 km in the south polar region to about 5000 km in the north polar region. Highest priority was assigned to the mapping sequences that were designed to obtain full coverage of the planet using the 50-mm focal-length camera. The characteristics of this camera and the footprint size as a function of distance are given in Table 1. Although this is the Mariner 9 wide-angle camera, its 10° × 14° field would normally be considered narrow-angle. In order to obtain coverage and keep the total number of pictures within reason, it was planned to use pictures taken from distances greater than 3500 km in the computation of the primary control net. In practice, this was not always possible. The secondary control net computations use mapping pictures exclusively.

The mission plan called for far-encounter pictures to be taken of the northern hemisphere before insertion into orbit. Pictures of the southern hemisphere were to be taken along the morning terminator early in the orbital mission in order to establish a quick preliminary control net. The dust storm that enveloped Mars at the time Mariner 9 arrived in mid-November 1971 caused a complete change in the plan. By January 1972, the dust had settled sufficiently to proceed with taking the geodesy sequence series of morning terminator pictures. Since November, however, the terminator had moved relative to the spacecraft's orbit, so it was necessary to take the sequence farther south in the orbit than was originally planned. The consequence is that these pictures are usable from about 70° to about 25° south latitude. The longitude coverage is good except for two gaps at about 90° and 270° due to the loss of data during a snowstorm at the Goldstone antenna.

Because many pictures of the south polar region were taken to monitor changes to the cap, the coverage there is good. The band from 25° south latitude to the equator contains pictures from the mapping sequence only. The sequences in this band, designed for full planetary coverage at maximum resolution, were taken near periapsis along the evening terminator. There is too little overlap between frames in these mapping sequences and the area covered per frame is too small for triangulation, thus requiring many frames for full coverage and resulting in gaps in the control net. For control purposes, special pictures were taken of the band from the equator to 20° north. North of 20° north, mapping pictures are used for control because the spacecraft was far from periapsis when they were taken.

During the next few years, many new charts and maps of Mars will be made, including large-scale maps that portray relatively small regions of the martian surface that contain few or no control points from the planet-wide net. A secondary control net, consistent with the primary net but with control points more closely spaced, will then have to be established in the area of interest. Although secondary control has not been required yet, the method of photogrammetric reduction has been prepared and tested.

After discussing the photogrammetric equations and the computational method used to establish the planet-wide control net and the secondary net, the camera stations and the assumed physical properties of Mars are considered. Subsequent paragraphs contain a description of the control points, their measurements, and a discussion of how distortions are removed. Finally, results of the computations are given, with tables of coordinates for the control points.

II. REDUCTION METHODS

The Primary Control Net

Determination of the positions of reference points in the primary network on the surface of Mars is essentially an exercise in analytic multiphotograph stereophotogrammetry, with important inputs from classical astronomy and the electronic sciences. Following selenodetic practice, the reference points are usually small, well-defined craters that are easily bisected and that show relatively small phase effects.

Measurements of the control points are discussed later in this paper. The pixel counts are reduced to millimeters, corrected for optical and electronic distortions, and the origin translated to the principal point, thus deriving the observed coordinates x_o, y_o. The focal length of the lens is f.

The stereophotogrammetry is peculiar in that the camera (spacecraft) positions come from the tracking data and are not determined in any way from the photogrammetry. The spacecraft positions could be adjusted for consistency using the photogrammetric data; however, since the camera has a narrow cone angle, the solutions for the spacecraft position and orientation would be highly correlated. Thus, it was necessary to hold one fixed, and, because the a priori position data appear much better than the angular data, the position values provided by the JPL Science Data Team were used without change.

The geometric visualization of the computations is that the rigid perspective cones derived from the (x_o, y_o, f) arrays for each picture are rotated about fixed vertices and oriented so that each set of corresponding rays meet as nearly as possible in one point. Corresponding rays are those derived from the same martian surface point. The photogrammetric operation thus produces a scaled model of Mars in the form of an aggregate (X_i, Y_i, Z_i) of coordinated points.

The method of analysis may appear awkward in some ways; however, the coordinate systems are compatible with those used at JPL, permitting easy exchange of data. Also, the method is completely general, permitting a convenient solution for the spin axis of Mars as well as control point coordinates and camera orientation angles.

The computations involve four distinct three-dimensional coordinate systems XYZ, X'Y'Z', X"Y"Z", and $\xi\eta\zeta$. All the XYZ systems are Mars centered, but the first of these, XYZ, rotates solidly with Mars and is valid for fixed martian surface coordinates. For this system we can write

$$X = R \cos \phi \cos (360° - \lambda),^{*} \tag{1}$$

$$Y = R \cos \phi \sin (360° - \lambda), \tag{2}$$

$$Z = R \sin \phi, \tag{3}$$

where R is the length of the areocentric radius to the surface point in kilometers, ϕ is the latitude of this radius (its inclination to the Mars equatorial plane), and λ is the west areocentric longitude measured from the positive X-axis.

The nonrotating or inertial system X'Y'Z' is such that the X'-axis is directed through the ascending node of the Mars mean equator on the mean ecliptic of 1950.0. The Y'-axis is on the Mars equator.

The inertial system X"Y"Z" has its X"-axis in the plane of the Earth mean equator of 1950.0 through the vernal equinox. The Y"-axis is on the Earth mean equator.

---

*(360° - λ) is used instead of λ to make the coordinate system right-handed.

The system $\xi\eta\zeta$ uses the coordinate axes of the camera but applied to Mars surface points. The origin is the spacecraft.

If V is the hour angle of the mean equinox measured from the prime meridian, then the coordinates of a surface point in the X'Y'Z' system are

$$\begin{bmatrix} X' \\ Y' \\ Z' \end{bmatrix} = W \begin{bmatrix} X \\ Y \\ Z \end{bmatrix}, \tag{4}$$

where

$$W = \begin{bmatrix} \cos V, & -\sin V, & 0 \\ \sin V, & \cos V, & 0 \\ 0, & 0, & 1 \end{bmatrix}. \tag{5}$$

Now let M be the 3×3 orthogonal matrix representing the rotation from the Mars-centered inertial system X'Y'Z' oriented on the Mars equator to the second Mars-centered inertial system X"Y"Z" oriented on the 1950.0 Earth mean equator. Then

$$\begin{bmatrix} X'' \\ Y'' \\ Z'' \end{bmatrix} = M \begin{bmatrix} X' \\ Y' \\ Z' \end{bmatrix} = MW \begin{bmatrix} X \\ Y \\ Z \end{bmatrix}. \tag{6}$$

Since the spacecraft positions are S_x, S_y, S_z in the X"Y"Z" system, the coordinates of the surface point with the spacecraft as origin are

$$\begin{bmatrix} X'' \\ Y'' \\ Z'' \end{bmatrix} - \begin{bmatrix} S_x \\ S_y \\ S_z \end{bmatrix},$$

and if the 3×3 orthogonal matrix C represents the rotation from the X"Y"Z" system to the photographic system, then we have

$$\begin{bmatrix} \xi \\ \eta \\ \zeta \end{bmatrix} = C \begin{bmatrix} X'' \\ Y'' \\ Z'' \end{bmatrix} - C \begin{bmatrix} S_x \\ S_y \\ S_z \end{bmatrix}$$

$$= CMW \begin{bmatrix} R \cos\phi \cos(360° - \lambda) \\ R \cos\phi \sin(360° - \lambda) \\ R \sin\phi \end{bmatrix} - C \begin{bmatrix} S_x \\ S_y \\ S_z \end{bmatrix}. \qquad (7)$$

where ξ, η, ζ, are the coordinates of the surface point in the photographic system with the spacecraft as origin. Now,

$$\frac{x}{f} = \frac{\xi}{\zeta} , \quad \frac{y}{f} = \frac{\eta}{\zeta}$$

where f is the calibrated principal distance. Thus

$$x_c = \frac{\xi f}{\zeta} , \quad y_c = \frac{\eta f}{\zeta} . \tag{8}$$

The subscript c emphasizes that x_c and y_c, derived in this way from assumed R, ϕ, λ, are <u>computed</u> values as distinct from the observed values x_o, y_o.

Whereas the computation of x and y from R, ϕ, λ is direct, the reverse computation, which is what interests us, involves the solution of transcendental equations. The solution given in this paper is the usual method of iteration in which the discrepancies are computed rigorously using Equations (7) and (8). These are then used in the solution of approximate linear equations to compute the first-order corrections to the unknown parameters. For a point i imaged on picture j, the linear observation equations are

$$\sum_i \frac{\partial x_{ij}}{\partial P_i} \cdot \Delta P_i + \sum_k \frac{\partial x_{ij}}{\partial P_{jk}} \cdot \Delta P_{jk} = \left(x_o - x_c\right)_{ij} , \tag{9}$$

$$\sum_i \frac{\partial y_{ij}}{\partial P_i} \cdot \Delta P_i + \sum_k \frac{\partial y_{ij}}{\partial P_{jk}} \cdot \Delta P_{jk} = \left(y_o - y_c\right)_{ij} , \qquad (10)$$

in which the P_i are the parameters defining the position of i, and the P_{jk} are the parameters (k = 1, 2, 3) defining the orthogonal matrix C_j. The subscripts o and c indicate observed and computed values, and the subscript ij indicates point i on picture j.

The matrix C is derived from the tracking data plus the telemetered clock and cone angles. However, it does not always have a precision commensurate with the other data and hence, in general, is merely used as a starting value in the iterations.

The photogrammetric method is general and, in principle, can be used to solve for almost any of the parameters. As the Mariner television pictures are poor for photogrammetric use and as they were frequently taken at non-optimum times for this purpose, it is desirable to minimize the number of variables in the solution. Thus, the camera stations (S_x, S_y, S_z) are taken from the Supplementary Experiment Data Record (SEDR), which is published by the Science Data Team at JPL. The accuracy of these coordinates of the spacecraft position is expected to be about 3 km in each direction. In all computations, the three angles that define the camera orientation matrix C are treated as variables and are part of the solution. The latitude and longitude of the control points are always variables; however, the vector radius R has usually been derived from the radio occultation experiment [Kliore et al., 1972]. The only exception is in the region of Nix Olympica, where there was a deliberate effort to determine the altitude of the mountain photogrammetrically.

Because of the narrow cone angle of the camera, there usually are not adequate parallactic angles between successive exposures to obtain planetary radii measurements from the photogrammetric solution. Thus, they were principally derived from the radio occultation radii measurements.

The radius of each control point is the sum of the radius of the reference spheroid at the point's latitude and longitude and the elevation above the reference spheroid linearly interpolated from Table 2. The elevations in Table 2 are interpolated from the elevations at the occultation points given by Kliore et al. [1972]. In this table the elevation is assumed to be zero at the north pole and south at 65° south latitude, as there are no measurements reported south of 40° south.

Thus, each picture contributes three unknowns -- the parameters of C; each point contributes two unknowns -- ϕ and λ; and each observed image contributes two equations. Generally, three iterations are sufficient to attain stationary state in the solution.

The least-squares solution, which minimizes discrepancies in the picture plane, is general and does not distinguish between observations, unknown parameters, and a priori knowns. All become unknowns with appropriate weights. This give the program considerable flexibility in regard to holding values fixed or permitting them to vary.

One of the principal problems is the size of the equation set to be solved. Because it is not feasible to attempt the simultaneous solution for the coordinates of all vertices of the primary triangulation, we have had to work in blocks. Adjustments between blocks have been made using common points and holding one block fixed in each adjustment. The procedure is far from perfect, but unfortunately the optimum procedure does not lie in the realm of practical economics.

The Secondary Control Net

The Mars secondary control net (triangulation), like its terrestrial counterparts, is intended to fill the interstices of the primary net with a much denser network of controls. Again, like its terrestrial parallels the Mars secondary net is less complex, and its reductions are much less expensive than those of the primary net.

The primary network involves three unknowns per picture and two unknowns for each point fixed. In contrast, the secondary net determination involves four unknowns* per photograph, but no additional unknowns for points. In addition, because of its subsidiary and dependent nature, reduction and adjustment of the secondary net can be split into blocks, thus bringing the computation problem down to a manageable size.

The standard block size has been set up as 40 pictures (160 unknowns). Each USGS 1:5,000,000 Mars chart will contain four or more blocks.

---

*These unknowns are the coefficients of the general two-dimensional transformation of rectangular coordinates.

The materials used in the primary and secondary triangulations are substantially different. Whereas uncorrected pictures, frequently small-scale, were used in the primary work, with pixel counts to establish positions in the images, the secondary net is based on the use of rectified picturs, which are measured in ordinary two-coordinate comparators. The rectified pictures are the result of extensive processing at the Image Processing Laboratory (IPL) of the Jet Propulsion Laboratory. The method of producing the rectified pictures has been reported by Gillespie and Soha [1972], and the programs and the parameters used in the Mariner 9 project are discussed by Rofer [1972, unpublished data]. The pictures are enhanced, corrected for electronic distortion, mathematically transformed into map fragments according to definite map projection formulas, and finally stored in this form on magnetic tapes. They are then converted into actual negatives with the Optronics Photowrite of the Center of Astrogeology, in Flagstaff, Arizona.

Although the Optronics equipment reproduces precisely what is on the tape, our measuring routines are intended to control errors arising from those imperfections that must occur in practice. Six marginal marks with known pixel counts in x and y are always included in the measures. Thus, all measurements can always be converted into pixel counts with fair precision.

As our measurements are on rectified pictures that are regarded as map fragments, it should be clear that the secondary triangulation is performed in the map plane. This practice is not at all unusual in the major geodetic establishments. The theory of the adjustment is very simple. Each mosaic element, regarded as a map fragment, is shifted, rotated, and dilated in such a manner that the discrepancies in x and y at the tie points are minimized. These points are generally very small craters, but we have also used angles in shadows and ridges. Even with these angles it is frequently impossible to find common points between adjacent pictures, so that the fixation routes become somewhat dendritic. An adjustment such as the above can be represented by the general transformation of rectangular coordinates in two dimensions.

$$X = px - qy + a$$

$$Y = py + qx + b$$

where (x, y) is a position on the mosaic element and (X, Y) the corresponding map position. The above become the observation equations for control points. For a tie point i on pictures j, k, the observation equations are

$$p_j x_{ij} - q_j y_{ij} + a_j - p_k x_{ik} + q_k y_{ij} - a_k = 0$$

$$p_j y_{ij} + q_j x_{ij} + b_j - p_k y_{ik} - q_k x_{ik} - b_k = 0$$

The normals are formed and solved by the usual methods. Residuals are computed in order to monitor quality. As already noted, the programs for the USGS IBM 360/65 computer can handle 40 pictures in one adjustment. The 1:5,000,000 scale chart may contain at least twice this number of pictures, so subsidiary adjustments will generally be necessary to adjust the blocks to consistency. Figure 1 is a sample layout of the secondary net for one of these charts.

Because most of the tie points are small and possibly elusive as to identity, the measures and reductions also carry one distinct and well-defined crater for each picture, placed as nearly as possible at the center of the picture. These are the secondary controls. At this point it would be dangerous to predict their quality, but their absolute precision should not be appreciably inferor to those of the primary points, and their relative precision, the local positional consistency, should be better.

III. MARINER 9 CONTROL NET PARAMETERS

A specific set of constants defining the areographic coordinate systems has been adopted by the Mariner 9 Geodesy/Cartography Group of the Television Team, and these values are used for all Mariner 9 cartographic products. This coordinate system, its derivation, and its rationale are discussed in de Vaucouleurs, et al. [1973] and the spin axis, prime meridian, and reference spheroid for the maps are defined. These are used in the control net computations and provide the surface feature coordinates to the cartographers in a usable form.

Using the notation of Sturms [1971], with T as the time in Julian centuries from the epoch 1950, January 1.0, E.T. (Julian date 2433282.5), the right ascension and declination of the martian pole are:

$$\alpha_{50} = 317\overset{\circ}{.}32 - 0.1011\ T\ ,$$

$$\delta_{50} = 52\overset{\circ}{.}68 - 0.0570\ T\ .$$

The matrix M, which relates the Mars-equatorial coordinate system to the 1950.0 Earth-equatorial coordinate system on January 1.0, 1971 (Mariner 9), thus has the numerical value

$$M = \begin{bmatrix} -0.09879443, & 0.88973139, & 0.44566546 \\ -0.90538578, & 0.10547699, & -0.41127994 \\ -0.41293612, & -0.44413134, & 0.79512962 \end{bmatrix} .$$

The prime meridian is now defined as passing through the center of the crater, provisionally designated Airy-0, that lies in the large crater provisionally called Airy. Airy-0 is seen on narrow-angle frame number 533-3 (MTVS 4296-118, CAS 13165361) (the frame number refers to the third frame taken on revolution 533). The control net position, particularly the position of Airy-0, must now be used to adjust the added constant in the angle V that is measured from the Mars vernal equinox to the Mars prime meridian along the equator. Thus, the adjusted value of V is

$$V = 148\overset{\circ}{.}68 + 350\overset{\circ}{.}891962\ (JD - 2433282.5)\ .$$

The computations are performed entirely in terms of areocentric coordinates, that is, in terms of the latitude ϕ, the longitude λ, and the length R of the radius from the center of Mars through the point. All Mariner 9 map products will use areographic coordinates in which the latitude ϕ' of a point is defined as the angle between the equatorial plane and the normal to the reference spheroid at the point. These planetographic coordinates are appropriate when the local vertical is used as a reference direction, such as on the surface of Earth, and they will therefore be relevant to the operation of landers and rovers on Mars. The adopted reference spheroid has an equatorial radius a of 3393.4 km and a polar radius c of 3375.8 km.* If a point lies on the spheroid, the areocentric and areographic latitudes are related by

$$\tan \phi = \left(\frac{c}{a}\right)^2 \tan \phi' .$$

---

*These values of a and c were used in the reduction of the Mariner 6 and 7 pictures [Davies, 1971]; at a meeting of the Geodesy/Cartography group on March 28, 1972, it was decided that the same values should be used in the reduction of the Mariner 9 pictures after discussions of the new data available regarding the shape of the planet [de Vaucouleurs, et al., 1973].

IV. THE CONTROL POINTS

The control points are chosen on the basis of several criteria. The point must be uniquely related to a topographic feature, and often it is defined as the center of a small crater. It must be a point on the solid surface; care must be taken to avoid using points that are associated with clouds or ice, as they might be difficult to find in the future. Each point must be found on at least two pictures and, if possible, more. Each picture in the net must contain more than two points. Thus, the points must be close together when the picture covers a small area, and the craters can then be small because the resolution is good. On the other hand, a large number of frames must be used to cover a specific area. Thus, the planet-wide density of control points reflects the surface coverage of individual frames; this effect is seen in Figure 2, which shows the locations of all points of the primary net. In the future, effort will be made to reduce the size of the gaps by adding more points and pictures to the net.

To use the control net, it is necessary to identify the control point on the pictures and then to refer to its coordinates in the tables given in the next section of this paper. As the primary net is derived from several hundred frames, it is not practical to publish all of them with the points identified. However, most of the points have been located on a series of 1:5,000,000 uncontrolled photomosaics compiled by the U.S. Geological Survey and are seen in Figures 3 through 31. The numbers of points not identified on these maps are given in Table 3.

For the primary net, the measurements of the points are made by counting pixels (picture elements) on pictures that have had no geometric processing. The IPL produces special versions of the frames for this purpose; they are high-pass filtered and stretched, and a special counting grid is incorporated to help in pixel counting. The IPL uses a computer program to locate, in pixel coordinates, the 195 reseau points on each picture. During calibration before launch, the locations of the reseau points on the vidicon tube were carefully measured using an optical comparator, and the optical and geometric distortions relative to the reseau points were measured using special targets in the collimator. The data was used by Kreznar [1972, unpublished data] to prepare a program to remove the distortions when the reseau point locations were known. This program was used to transform the control point measurements in pixel coordinates into image coordinates (in millimeters), with the origin at the principal point of the optics. The pixel coordinates of each point on each frame are measured three or four times by two or three different persons. Any measurement differing from the median measurement by more than two pixels is rejected (as a gross error) and the pixel coordinates ($\overline{X}$, $\overline{Y}$) are the mean of the remaining measurements. Each individual measurement is estimated to the one-tenth pixel; the standard error of the mean is usually between 0.2 and 0.5 pixel (0.003 to 0.007 mm). This program, which transforms pixel coordinates ($\overline{X}$, $\overline{Y}$) into image coordinates (x_o, y_o), is essentially the same as the one used by the IPL to produce their geometrically corrected pictures.

Measurements for the secondary triangulation are made differently. A positive or negative of the picture is measured directly on a Mann two-coordinate monocomparator. The picture is then produced, as stated earlier, at the U.S. Geological Survey in Flagstaff, Arizona, on an Optronics Photowrite machine from a rectified magnetic tape supplied by the IPL. These pictures are produced at USGS rather than at the IPL/JPL because all the video film converters at the IPL use cathode-ray tubes, which introduce their own geometric distortions. This is the reason that the measurements for the primary net are made by pixel counting instead of measuring film with a comparator.

The crater Airy-0, which now defines the prime meridian, is identified on the narrow-angle picture mentioned above, but it is too small to be seen on wide-angle pictures. The primary control net is composed entirely of wide-angle pictures in order to maximize surface coverage, so it is necessary to determine the coordinates of Airy-0 on a wide-angle picture that also contains other points of the net. Wide-angle frame 533-1 (MTVS 4296-111, DAS 13165256) was taken at about the same time as frame 533-3, so that the viewing and lighting geometry of the low-resolution and high-resolution frames are similar. Alan Gillespie of the IPL and Gordon Hoover of the California Institute of Technology independently transferred the point (Airy-0) from the narrow-angle frame and determined the pixel coordinates. This is more difficult than would appear at first because the narrow-angle frames are rotated 60° relative to the wide-angle frames, and there is a great deal of scale distortion in the uncorrected frames (because the horizontal and vertical pixel sizes are not the same on the vidicon camera, but are the same on the IPL video-film-converter versions of the pictures).

Gillespie transferred the position of Airy-0 from frame 533-3 to 533-1 using the IPL machine-matching program as well as by eye through interpolation between points common to both frames. Hoover transferred the point by eye to this frame and also to other frames containing this region. These measurements are summarized in Table 4. It is felt that the machine-matching program gives the best results, so those measurements on 533-1 are used to define the prime meridian for the control net. The difference in longitude between this measurement and other measurements on 533-1 and other frames are given in Table 4; the standard error of transfer was about $0\overset{\circ}{.}014$ longitude.

V. THE COMPUTATIONS

The effort on the primary net has been to add points and pictures to cover the entire surface of the planet. At this time, the net contains 1205 points on 598 frames and is planet-wide; however, some large gaps still exist. Future work will be aimed at reducing the gaps.

Work on the secondary net is about to start, and there are no specific results to report at this time. This triangulation is particularly important to fill gaps in the primary net and to increase the density of control points in particular regions used in the preparation of a large-scale map.

The number of points and frames now in the primary net is so large that the control computations have been divided into five overlapping blocks. The coordinates of the points in each block are computed as independent adjustments; however, in the overlap regions a few points are held at positions determined by the adjustment of the neighboring block. The block solution is iterative and the computations are continued until all of the point coordinates in the overlapping regions do not change. Usually two to three adjustments of each block are required for the solution. A summary of these results is given in Table 5. The areographic coordinates of the points are given in Table 6.

It is always difficult to estimate the accuracy of coordinates because frequently unknown systematic errors are more important than the standard errors that come from the computations. At this stage of the work, the random horizontal error is thought to be about 10 km. To this must be added a regional error that is a function of position; near Airy-0 this type of error is very small whereas at the antipode of Airy-0 it may be as large as 20 km. This error will also be high, perhaps 15 km to 20 km, for those coordinates whose points lie on the periphery of the gaps in photographic coverage.

ACKNOWLEDGMENTS

We appreciate the counsel and cooperation of Harold Masursky and all members of the Mariner 9 Television Team. Particular thanks go to Gerard de Vaucouleurs, Raymond Batson, and Warren Borgeson of the Geodesy/Cartography Group.

We thank Gordon Hoover and Tav Heistand of Caltech and Rose Heirschfeldt of the Rand Corporation for measuring the coordinates of the points on the pictures, and to Frank Katayama of the Rand Corporation for managing the computer operations used in the primary control net.

William Green, Joel Seidman, and many other members of the Image Processing Laboratory at JPL deserve special thanks for furnishing versions of the pictures and tapes that made this work possible.

Michael Sander and members of the Mariner 9 Science Data Team at JPL have been helpful in supplying SEDR coordinates of the picture stations. Francis Sturms, Jr., of JPL deserves thanks for computing the new M matrix and other parameters which changed with the introduction of a new spin axis for Mars.

This research was supported by the Jet Propulsion Laboratory, California Institute of Technology, through Rand Contract No. 953011 and WO-8122 with the U. S. Geological Survey.

Table 1

MARINER 9 WIDE-ANGLE TELEVISION CAMERA

Sensor - slow scan vidicon
Optics - Zeiss Planar, 52.267-mm focal length, f/2 stopped down to f/4
Format - 9.6 mm × 12.5 mm, 700 × 832 pixels
Field of view - 11° × 14°

Normal Distance to Plane Surface (km)	Pixel Size (km)	Footprint (km)
2000	0.56	380 × 500
3000	0.84	580 × 750
4000	1.1	770 × 1000
5000	1.4	960 × 1250
6000	1.7	1150 × 1500

Table 2

SURFACE ELEVATIONS ABOVE REFERENCE SPHEROID AT 10° INTERVALS (AREOCENTRIC)
(Derived from occultation experiment radii)
(in kilometers)

Latitude	West Longitude																	
	170	160	150	140	130	120	110	100	90	80	70	60	50	40	30	20	10	0
90	0.0	0.0	0.0	0.0	0.0	0.0	0.0	0.0	0.0	0.0	0.0	0.0	0.0	0.0	0.0	0.0	0.0	0.0
80	-1.01	-1.07	-0.86	-0.74	-0.69	-0.06	-0.51	-0.54	-0.53	-0.78	-0.87	-1.07	-1.19	-1.12	-1.16	-1.07	-0.89	-0.89
70	-2.02	-2.13	-1.71	-1.47	-1.38	-0.12	-1.00	-1.08	-1.05	-1.55	-1.74	-2.15	-2.38	-2.23	-2.32	-2.15	-1.78	-1.78
60	-2.39	-1.91	-1.51	-1.37	-0.92	-1.18	-0.91	-0.91	-1.07	-0.92	-1.32	-2.04	-2.82	-2.95	-3.03	-2.83	-2.36	-2.05
50	-2.08	-1.75	-1.61	-1.47	-0.12	0.26	0.38	0.23	0.39	0.58	-0.51	-0.92	-1.63	-2.12	-2.37	-2.47	-1.83	-1.59
40	-1.77	-1.81	-0.70	-1.59	0.68	1.77	1.83	1.68	1.62	1.76	0.34	-0.27	-0.67	-1.53	-1.79	-1.47	-1.31	-1.15
30	-1.72	-1.72	-0.14	0.32	1.48	3.29	3.29	3.14	2.86	2.94	1.19	0.39	0.29	-0.94	-1.44	-0.87	-1.01	-0.69
20	-1.73	-1.96	0.43	1.14	3.61	4.22	4.69	4.16	4.19	3.32	2.82	1.99	0.56	0.08	-0.68	-0.36	-0.38	-0.23
10	-0.74	-0.53	0.24	1.97	4.45	5.32	6.14	5.61	5.44	4.25	3.65	2.70	1.56	1.03	0.09	0.15	0.25	0.23
0	0.68	0.38	1.54	3.27	5.29	6.42	7.60	7.06	6.70	5.18	4.48	3.41	2.56	1.97	0.85	0.64	0.99	1.05
-10	1.99	1.71	2.67	4.36	6.23	7.52	9.05	8.51	7.94	6.07	4.68	4.27	3.35	2.24	1.19	1.07	1.80	1.82
-20	3.30	3.04	3.79	4.56	6.60	8.48	6.78	9.06	8.24	6.17	5.61	4.24	3.21	2.42	1.76	1.50	2.60	2.59
-30	3.21	2.99	4.38	4.13	6.68	6.66	7.54	9.37	8.46	6.67	6.60	4.89	3.30	2.79	1.98	2.55	2.05	2.55
-40	2.29	2.14	2.11	5.14	4.12	5.92	6.41	5.64	6.76	5.21	4.35	3.52	2.36	1.99	1.42	1.82	1.47	1.82
-50	1.37	1.28	1.27	3.08	2.47	3.55	3.85	3.39	4.05	3.13	2.61	2.11	1.41	1.19	0.85	1.09	0.88	1.09
-60	0.46	0.43	0.42	1.03	0.82	1.10	1.28	1.13	1.35	1.04	0.97	0.70	0.47	0.40	0.28	0.36	0.29	0.36
-70	0.0	0.0	0.0	0.0	0.0	0.0	0.0	0.0	0.0	0.0	0.0	0.0	0.0	0.0	0.0	0.0	0.0	0.0
-80	0.0	0.0	0.0	0.0	0.0	0.0	0.0	0.0	0.0	0.0	0.0	0.0	0.0	0.0	0.0	0.0	0.0	0.0
-90	0.0	0.0	0.0	0.0	0.0	0.0	0.0	0.0	0.0	0.0	0.0	0.0	0.0	0.0	0.0	0.0	0.0	0.0

Latitude	West Longitude																	
	350	340	330	320	310	300	290	280	270	260	250	240	230	220	210	200	190	180
90	0.0	0.0	0.0	0.0	0.0	0.0	0.0	0.0	0.0	0.0	0.0	0.0	0.0	0.0	0.0	0.0	0.0	0.0
80	-0.94	-0.34	-0.69	-0.79	-0.71	-0.31	-0.26	-0.61	-0.64	-0.65	-0.58	-0.70	-0.86	-1.03	-1.34	-1.03	-0.96	-0.97
70	-1.86	-1.67	-1.38	-1.58	-1.42	-0.62	-0.52	-1.21	-1.28	-1.30	-1.16	-1.41	-1.72	-2.07	-2.68	-2.06	-1.92	-1.95
60	-0.57	-1.74	-0.92	-1.36	-1.46	-1.34	-1.50	-1.50	-1.52	-1.55	-1.72	-1.86	-1.54	-1.86	-2.80	-2.14	-2.20	-2.15
50	-0.24	-1.11	-0.30	-0.58	-0.64	-0.76	-0.73	-0.98	-0.17	-1.09	-1.44	-1.59	-1.96	-1.80	-1.46	-1.77	-1.78	-1.65
40	-0.75	0.24	0.36	-0.04	0.19	0.06	0.11	-0.15	0.74	-0.08	-0.58	-0.77	-0.94	-1.46	-1.16	-1.55	-1.46	-1.44
30	-0.12	0.78	1.18	0.65	0.48	0.89	0.94	0.68	1.65	1.33	0.32	-0.21	-0.45	-1.12	-0.87	-1.27	-1.59	-1.43
20	0.51	1.36	1.98	1.66	1.20	1.78	1.61	2.51	1.73	2.17	1.16	0.76	-0.04	-0.81	-0.92	-1.07	-1.42	-1.40
10	1.27	2.46	2.60	2.49	1.92	2.59	2.44	3.31	2.71	3.00	2.04	1.74	0.37	-0.46	-0.75	-0.88	-1.24	-1.36
0	2.12	2.94	3.17	2.72	2.71	3.41	3.26	4.10	3.69	3.84	2.90	2.71	0.77	-0.12	0.05	0.0	-0.32	0.12
-10	3.00	3.43	4.08	3.72	3.27	4.22	4.09	4.90	4.67	4.53	3.44	3.36	2.26	1.50	1.50	1.97	1.98	1.14
-20	3.91	4.33	4.58	3.78	3.79	2.55	2.10	2.95	2.96	4.03	3.69	3.67	4.04	2.58	2.70	3.14	3.19	2.59
-30	3.15	3.46	3.51	4.22	3.03	-1.28	-1.47	-0.09	1.03	2.39	3.58	3.96	4.19	3.75	3.25	3.82	3.25	2.57
-40	2.25	2.47	2.51	3.62	-0.96	-3.38	-3.03	-1.17	0.20	1.53	2.65	2.83	2.99	2.68	2.32	2.73	2.32	1.84
-50	1.35	1.48	1.50	2.17	-0.57	-2.03	-1.62	-0.70	[illegible]	0.92	1.59	1.70	1.79	1.61	1.39	1.64	1.39	1.10
-60	0.45	0.49	0.50	0.72	-0.19	-0.68	-0.61	-0.23	0.04	0.31	0.53	0.57	0.60	0.54	0.46	0.55	0.46	0.37
-70	0.0	0.0	0.0	0.0	0.0	0.0	0.0	0.0	0.0	0.0	0.0	0.0	0.0	0.0	0.0	0.0	0.0	0.0
-80	0.0	0.0	0.0	0.0	0.0	0.0	0.0	0.0	0.0	0.0	0.0	0.0	0.0	0.0	0.0	0.0	0.0	0.0
-90	0.0	0.0	0.0	0.0	0.0	0.0	0.0	0.0	0.0	0.0	0.0	0.0	0.0	0.0	0.0	0.0	0.0	0.0

Table 3

CONTROL POINTS WHICH ARE NOT LOCATED ON THE USGS MOSAICS

0	761	1394	1598
27	762	1395	1599
187	766	1402	1600
192	813	1403	1602
196	863	1405	1605
197	865	1408	1608
234	891	1424	1611
236	938	1425	1612
243	946	1455	1614
246	948	1461	1616
271	949	1462	1617
276	950	1469	1618
279	951	1470	1619
306	954	1471	1620
316	957	1472	1621
335	959	1473	1622
338	963	1490	1623
358	977	1508	1624
368	1025	1514	1634
401	1026	1532	1635
403	1028	1533	1636
433	1039	1534	1640
476	1040	1535	1641
479	1053	1536	1646
481	1200	1537	1648
484	1240	1539	1649
485	1244	1545	1651
486	1268	1565	1652
494	1278	1569	1653
496	1285	1571	1654
498	1289	1573	1655
595	1291	1574	1678
615	1300	1577	
645	1308	1578	
654	1328	1580	
699	1329	1581	
701	1330	1582	
703	1340	1583	
704	1346	1586	
706	1356	1587	
708	1357	1591	
756	1383	1595	
757	1387	1596	
760	1392	1597	

Table 4

TRANSFER OF THE LOCATION OF AIRY-0 TO LOW-RESOLUTION FRAMES

Frame Number	DAS	Source	Method of Point Transfer	Pixel Coordinates		Longitude Difference
				X	Y	Deg.
533-1	13165256	Gillespie (Machine)		396.36	474.22	0°
533-1	13165256	Gillespie (Eye)		396.83	474.43	0°005
533-1	13165256	Hoover (Eye)		396.9	474.8	0°006
137-30	06499678	Hoover (Eye)		561.0	314.4	0°029
139-15	06571008	Hoover (Eye)		563.5	138.8	0°009
180-17	08045768	Hoover (Eye)		52.3	528.5	0°003

σ = 0°014

Table 5

SUMMARY OF PRIMARY CONTROL NET COMPUTATIONS

Block	Number of Points	Number of Frames	Number of Equations	Number of Unknowns	Standard Error, σ (mm)
North polar	274	141	1652	971	0.0176
0° north	335	140	1657	1090	0.0301
180° north	363	140	1753	1146	0.0144
0° south	231	142	1584	888	0.0157
180° south	238	154	1514	938	0.0226

The areographic coordinates of the points are given in Table 6.

Table 6

AREOGRAPHIC COORDINATES OF THE CONTROL POINTS

Point	Latitude ($\phi'°$)	W.Longitude ($\lambda°$)	Elevation (km)
0	-5.11	0.0	1.44
26	-15.75	3.67	2.24
27	-14.47	2.39	2.15
28	-20.36	4.31	2.57
31	-5.88	358.86	1.60
33	-4.03	356.37	1.76
34	-6.65	0.36	1.70
35	-4.71	2.64	1.40
37	0.72	358.51	1.13
38	-3.81	0.99	1.34
49	-77.08	0.77	-0.00
66	-80.27	353.43	-0.01
70	-75.69	323.93	-0.01
71	-75.38	307.37	-0.01
138	-79.72	329.76	-0.01
147	-69.64	42.70	0.02
148	-66.97	56.87	0.21
149	-71.18	26.49	-0.00
150	-41.81	7.26	1.46
153	-37.72	2.93	1.87
160	-81.07	340.63	0.00
161	-78.08	358.88	0.0
162	-74.02	323.90	-0.01
163	-78.71	143.16	-0.01
166	-72.22	176.11	-0.01
167	-72.18	163.71	-0.01
171	-72.67	257.97	-0.01
172	-72.79	264.49	-0.01
176	-83.29	353.15	-0.00
177	-81.24	19.37	-0.00
180	-48.95	10.48	0.96
181	-39.71	16.31	1.72
182	-53.74	32.39	0.71
183	-48.05	20.05	1.24
187	-33.34	75.36	6.09
190	-42.33	67.97	3.85
191	-43.81	60.22	3.05
192	-51.97	56.88	1.69
193	-50.28	72.70	2.76
194	-45.37	74.11	3.76
196	-80.94	48.59	-0.00
197	-82.29	73.46	-0.00
198	-67.02	17.23	0.11
199	-69.58	146.07	0.03

Table 6 (continued)

Point	Latitude ($\phi'°$)	W.Longitude ($\lambda°$)	Elevation (km)
200	-42.11	195.91	2.39
201	-50.06	190.91	1.45
202	-55.64	185.05	0.82
203	-50.40	175.49	1.22
204	-40.35	177.79	1.93
205	-26.61	188.30	3.13
206	-32.53	186.13	2.82
207	-33.73	202.67	3.27
208	-34.07	210.03	2.89
209	-27.11	217.08	3.30
210	-27.86	207.90	3.19
211	-33.14	227.42	3.72
212	-38.79	212.35	2.54
213	-43.26	225.57	2.50
214	-39.87	229.55	3.01
215	-23.19	237.42	3.80
216	-67.44	342.87	0.12
222	-75.94	289.37	-0.00
223	-80.68	289.58	0.00
224	-78.52	253.94	0.00
229	-70.65	349.64	-0.01
232	-69.20	359.43	0.02
233	-74.29	344.49	-0.01
234	-68.89	297.87	-0.09
236	-80.54	320.51	-0.00
237	-74.39	235.08	-0.01
238	-85.57	263.76	0.00
239	-78.12	230.46	-0.00
240	-75.94	210.70	-0.00
242	-63.98	317.44	0.31
243	-67.00	322.71	0.20
244	-70.82	311.43	-0.00
245	-64.83	312.24	0.00
246	-70.39	284.88	0.00
248	-62.14	148.47	0.40
249	-55.34	152.16	0.86
250	-60.57	142.09	0.84
251	-65.51	131.11	0.37
252	-65.08	121.90	0.54
253	-69.78	114.81	0.04
254	-68.48	97.43	0.19
255	-70.26	92.16	-0.00
256	-72.95	105.58	-0.00
257	-72.05	82.02	-0.00

Table 6 (continued)

Point	Latitude ($\phi'°$)	W.Longitude ($\lambda°$)	Elevation (km)
258	-72.13	131.76	-0.01
259	-77.19	128.37	0.00
261	-58.69	111.38	1.65
262	-53.26	125.01	2.33
263	-46.84	120.85	4.15
264	-42.66	119.74	5.27
266	-36.67	128.33	5.11
268	-55.61	78.12	1.96
269	-62.75	70.89	0.66
270	-62.46	44.08	0.33
271	-30.73	65.38	5.74
272	-38.13	52.91	2.94
273	-32.31	51.67	3.37
274	-20.32	45.75	2.90
275	-33.31	39.65	2.53
276	-42.81	34.41	1.50
277	-52.73	41.36	1.02
278	-30.44	25.87	2.19
279	-32.36	18.56	2.33
280	-39.01	25.65	1.66
281	-53.79	20.95	0.81
282	-60.04	23.45	0.34
283	-46.08	9.53	1.12
284	-63.92	259.28	0.19
285	-63.01	231.27	0.38
286	-48.94	260.04	0.95
289	-61.34	252.56	0.41
291	-32.88	245.36	3.43
292	-32.68	256.67	2.49
293	-49.30	237.75	1.81
294	-40.12	243.33	2.75
295	-49.23	218.97	1.69
296	-64.08	209.82	0.27
297	-27.82	233.13	4.03
298	-33.74	219.31	3.34
299	-43.78	215.13	2.15
300	-48.34	205.93	1.67
301	-44.48	203.40	2.14
303	-43.68	189.73	2.02
304	-64.03	196.90	0.32
305	-69.98	71.81	0.02
306	-77.03	71.44	-0.01
307	-53.28	197.01	1.26
309	-47.52	183.08	1.44

Table 6 (continued)

Point	Latitude ($\phi'°$)	W.Longitude ($\lambda°$)	Elevation (km)
310	-32.69	195.65	3.34
312	-61.03	177.02	0.36
313	-69.13	198.49	0.05
314	-32.48	175.85	2.64
315	-47.83	172.58	1.52
316	-33.23	165.79	2.87
317	-60.62	165.12	0.42
318	-46.73	162.03	1.64
319	-37.16	161.22	2.44
320	-42.32	131.99	3.99
321	-61.89	132.97	0.70
322	-34.12	151.54	3.32
323	-49.43	152.50	1.35
324	-55.25	155.92	0.87
325	-34.82	144.50	3.95
326	-31.36	159.91	2.91
327	-43.01	145.03	3.08
328	-55.61	136.45	1.86
329	-47.15	137.63	3.57
331	-33.97	11.66	1.91
334	-46.02	126.54	3.56
335	-34.04	0.18	2.24
336	-46.01	1.34	1.35
337	-56.18	8.53	0.54
338	-60.39	11.92	0.29
339	-28.18	2.08	2.45
340	-33.15	352.74	2.71
341	-47.92	345.71	1.61
342	-57.78	354.06	0.61
343	-35.06	339.04	2.98
344	-25.55	344.06	3.70
345	-23.40	352.57	3.36
346	-49.57	335.48	1.55
347	-61.52	338.90	0.42
348	-35.35	331.60	2.98
349	-24.71	332.96	4.03
350	-42.04	337.85	2.29
351	-46.67	325.05	2.26
352	-56.73	339.58	0.83
353	-59.24	322.57	0.78
354	-27.26	324.03	4.00
355	-35.76	322.79	3.61
356	-67.80	245.24	0.06
357	-70.73	327.75	-0.01

Table 6 (continued)

Point	Latitude (ϕ'°)	W.Longitude (λ°)	Elevation (km)
358	-65.51	335.34	0.22
359	-73.04	57.44	-0.00
361	-72.04	294.36	-0.00
362	-72.37	276.17	0.01
363	-68.87	216.78	0.06
364	-54.36	328.97	1.12
365	-69.26	45.52	0.04
366	-70.37	57.05	0.00
367	-73.53	316.94	-0.00
368	-80.29	82.19	-0.01
375	-57.42	312.80	0.11
376	-43.79	323.68	2.73
377	-43.55	315.32	1.33
378	-31.11	316.26	2.63
379	-34.14	314.57	1.68
380	-53.25	316.79	1.06
381	-45.77	304.84	-1.70
382	-77.47	54.58	0.00
383	-75.22	82.84	0.00
384	-73.07	100.01	-0.00
400	9.99	136.89	3.04
401	10.86	135.33	12.81
403	19.25	140.87	1.24
404	20.70	137.25	6.24
405	18.67	131.83	24.52
406	22.14	131.55	5.07
407	23.18	136.70	6.36
408	12.03	124.81	4.76
409	11.54	121.70	5.01
410	11.05	119.28	5.27
411	16.32	127.45	4.14
413	19.82	119.79	4.34
414	24.65	128.09	2.92
415	8.61	119.53	5.58
416	7.25	120.70	5.62
417	3.91	121.44	5.89
418	17.07	119.15	4.63
419	15.53	117.42	4.96
420	23.60	119.39	3.99
421	23.89	117.40	4.02
422	3.26	111.23	7.07
423	8.16	112.82	6.24
424	24.91	109.86	4.10
425	19.12	111.09	4.86

Table 6 (continued)

Point	Latitude ($\phi'°$)	W.Longitude ($\lambda°$)	Elevation (km)
426	17.78	114.15	4.87
427	9.41	102.20	5.89
430	8.81	112.16	6.21
433	11.37	97.46	5.44
435	18.26	95.18	4.48
436	22.14	103.28	4.18
437	25.35	102.51	3.79
438	25.58	98.85	3.66
439	24.53	91.59	3.67
440	26.74	92.13	3.41
442	28.51	87.78	3.10
443	24.55	89.78	3.65
444	22.11	89.32	3.95
445	21.57	80.97	3.37
446	13.10	83.30	4.38
447	13.67	79.84	3.95
449	4.34	82.62	5.19
450	16.73	82.27	3.91
451	20.23	77.21	3.20
452	28.44	79.49	2.98
453	25.41	81.06	3.19
454	11.47	76.92	3.97
455	1.07	72.04	4.54
456	7.63	72.97	4.04
457	11.70	72.44	3.67
458	11.30	69.07	3.47
459	20.03	71.92	2.95
460	18.05	72.60	3.14
461	19.45	68.45	2.76
462	26.91	71.17	1.93
463	23.24	72.23	2.53
464	20.68	64.20	2.27
465	25.21	63.67	1.50
466	16.67	64.30	2.62
467	11.26	64.44	3.04
468	6.69	64.22	3.37
470	12.72	60.72	2.58
471	20.70	58.56	1.72
472	13.18	54.05	1.76
473	10.06	55.41	2.19
475	11.43	50.75	1.52
476	16.44	54.40	1.52
477	20.04	56.25	1.47
478	23.00	55.96	1.12

Table 6 (continued)

Point	Latitude ($\phi'°$)	W.Longitude ($\lambda°$)	Elevation (km)
479	20.32	47.78	0.45
480	24.78	47.11	0.20
481	19.35	45.30	0.42
483	19.53	42.07	0.24
484	10.58	40.10	0.99
485	7.46	46.02	1.60
486	2.43	46.31	2.11
487	19.59	29.84	-0.63
488	10.79	34.90	0.49
489	12.01	25.42	-0.01
490	8.40	25.36	0.22
491	17.33	24.95	-0.35
492	19.87	24.05	-0.48
493	23.69	26.85	-0.83
494	26.91	25.80	-0.99
495	19.56	15.77	-0.34
496	25.30	17.51	-0.65
497	19.79	12.11	-0.36
498	19.19	20.01	-0.32
500	11.29	17.28	0.11
501	4.91	16.35	0.48
502	11.19	12.13	0.15
503	10.30	16.12	0.18
504	11.00	6.67	0.18
505	0.44	6.88	0.98
506	15.93	7.23	-0.10
507	19.11	7.48	-0.29
508	26.02	7.67	-0.69
509	18.48	2.67	-0.19
510	10.21	2.72	0.23
511	8.46	1.54	0.36
512	11.15	358.82	0.29
513	5.11	358.08	0.83
514	15.51	357.84	0.15
515	18.78	358.21	-0.04
516	13.48	355.31	0.51
517	8.94	355.11	0.82
518	5.91	354.41	1.14
519	11.53	354.72	0.69
520	18.39	353.25	0.38
521	15.06	355.12	0.43
522	15.48	350.86	0.78
523	0.35	2.74	1.01
524	2.27	2.54	0.86

Table 6 (continued)

Point	Latitude ($\phi'°$)	W.Longitude ($\lambda°$)	Elevation (km)
525	6.80	358.24	0.67
527	4.92	38.88	1.40
528	4.04	33.66	0.94
529	6.10	35.00	0.90
530	9.01	37.27	0.88
531	10.48	31.38	0.20
532	15.40	34.73	0.09
533	18.23	29.06	-0.51
534	12.57	30.98	-0.01
535	9.74	346.36	1.72
536	9.42	345.66	1.83
537	14.41	344.97	1.46
538	12.87	338.95	2.18
539	14.61	346.14	1.33
540	10.59	348.15	1.44
542	18.69	347.07	0.88
543	20.73	345.55	0.85
544	22.15	338.19	1.34
545	11.37	336.92	2.39
546	5.37	338.88	2.70
547	10.94	331.94	2.52
548	11.25	329.77	2.53
549	16.02	337.32	1.92
550	19.62	336.53	1.62
551	19.04	333.00	1.88
552	19.47	329.16	2.00
553	24.51	336.80	1.28
554	27.35	337.42	1.07
555	6.91	328.13	2.74
556	9.40	328.86	2.62
557	10.43	321.61	2.48
558	12.15	323.56	2.38
560	16.10	329.66	2.23
561	19.23	324.70	1.89
562	19.80	320.56	1.72
563	23.64	328.45	1.65
564	26.42	327.62	1.38
567	7.84	319.76	2.53
568	10.28	317.47	2.33
569	10.44	311.74	2.00
570	13.99	321.03	2.20
571	15.72	319.84	2.03
572	18.77	318.24	1.70
573	17.68	312.15	1.49

Table 6 (continued)

Point	Latitude ($\phi'°$)	W.Longitude ($\lambda°$)	Elevation (km)
574	22.32	321.10	1.49
575	25.90	318.73	1.25
577	7.87	312.34	2.21
578	5.25	311.40	2.35
579	12.45	309.70	1.77
580	12.42	305.74	2.02
581	11.55	302.62	2.30
582	12.42	311.99	1.87
583	15.17	312.35	1.68
584	21.90	312.43	1.18
585	26.23	310.84	0.79
586	20.17	305.97	1.43
587	21.38	307.07	1.27
588	19.67	301.33	1.74
589	6.52	303.94	2.60
590	9.28	303.28	2.43
591	10.12	301.44	2.49
592	10.06	295.75	2.53
593	9.11	294.34	2.59
594	15.13	303.49	1.96
595	18.73	303.15	1.70
596	18.27	298.05	1.91
597	18.12	294.83	1.86
598	23.57	304.07	1.26
599	26.87	300.62	1.16
600	23.92	293.39	1.39
601	25.82	294.51	1.25
602	19.11	296.40	1.81
603	19.30	286.13	2.02
604	18.59	289.18	1.81
605	13.94	293.93	2.19
606	10.02	287.60	2.65
607	10.75	290.68	2.39
608	4.73	294.21	2.94
609	1.49	296.48	3.24
610	6.96	285.51	3.08
611	3.07	285.73	3.37
612	11.37	285.37	2.74
613	11.14	280.72	3.15
614	11.26	277.22	3.05
615	17.29	286.38	2.17
616	13.82	285.65	2.51
617	20.08	283.42	2.20
618	19.78	278.63	2.44

Table 6 (continued)

Point	Latitude ($\phi'°$)	W.Longitude ($\lambda°$)	Elevation (km)
619	23.51	287.54	1.51
620	25.72	284.90	1.37
621	22.67	277.86	1.99
622	24.93	275.42	1.66
623	17.34	275.12	2.38
624	17.00	280.08	2.75
625	15.43	278.87	2.82
626	13.60	277.19	2.85
628	8.22	275.17	3.19
629	6.47	276.79	3.43
631	6.23	279.59	3.59
632	18.38	350.88	0.57
633	19.30	350.15	0.56
634	3.82	270.51	3.35
635	2.78	269.91	3.42
636	5.96	269.10	3.13
637	6.39	270.73	3.12
638	8.11	268.56	2.94
641	8.14	266.66	2.99
642	7.87	264.82	3.06
643	17.04	268.41	2.09
644	14.34	268.78	2.34
645	13.29	268.72	2.44
646	12.35	263.38	2.70
647	12.61	266.06	2.59
648	11.18	267.92	2.66
650	13.08	256.35	2.38
651	14.69	264.35	2.46
652	15.16	260.60	2.56
653	16.94	266.51	2.18
654	20.29	258.90	2.04
655	21.27	258.10	1.90
657	26.63	256.58	1.27
658	23.85	258.36	1.68
659	19.35	250.66	1.30
662	16.62	257.02	2.15
663	12.56	249.18	1.79
664	11.65	253.23	2.21
668	12.64	247.62	1.73
669	9.91	248.71	2.00
670	6.51	249.50	2.32
671	4.45	248.06	2.46
672	1.81	248.27	2.70
673	11.52	239.08	1.48

Table 6 (continued)

Point	Latitude ($\phi'°$)	W.Longitude ($\lambda°$)	Elevation (km)
674	11.28	244.64	1.76
675	15.81	248.90	1.50
676	17.20	249.58	1.40
677	20.49	241.17	0.77
678	20.19	243.71	0.90
679	20.08	246.34	1.02
680	21.62	248.78	0.97
681	23.61	250.06	0.87
682	26.13	249.38	0.63
684	22.75	238.92	0.44
685	23.33	242.07	0.54
686	25.70	239.76	0.22
687	18.07	242.00	1.03
688	17.17	236.12	0.87
689	17.11	231.86	0.28
690	13.18	241.76	1.49
691	15.35	240.26	1.23
692	10.01	238.94	1.61
693	9.08	241.02	1.86
694	8.56	236.92	1.44
695	8.51	231.53	0.67
696	6.27	239.71	2.07
697	2.11	242.68	2.55
698	1.74	240.75	2.56
699	9.85	230.98	0.53
700	5.89	231.26	0.75
701	12.32	229.70	0.26
702	12.33	221.09	-0.44
703	21.79	227.42	-0.29
704	21.23	224.77	-0.47
705	21.61	221.96	-0.69
706	29.88	229.41	-0.47
707	28.30	221.81	-0.92
708	29.13	228.25	-0.52
709	27.25	221.08	-0.94
710	9.67	221.39	-0.32
711	7.91	220.53	-0.33
714	2.14	221.32	-0.07
715	11.84	215.41	-0.63
716	12.02	213.31	-0.59
717	14.75	222.40	-0.41
718	20.35	220.58	-0.76
720	20.00	213.05	-0.86
721	24.73	221.63	-0.82

Table 6 (continued)

Point	Latitude ($\phi'°$)	W.Longitude ($\lambda°$)	Elevation (km)
722	23.67	211.53	-0.88
723	26.78	211.77	-0.89
724	27.53	208.27	-0.91
725	25.52	209.06	-0.89
726	26.56	202.31	-1.08
727	21.71	206.37	-0.95
728	20.79	200.78	-1.02
729	19.12	206.47	-0.91
730	17.38	200.16	-0.97
731	13.77	208.10	-0.80
732	13.14	205.27	-0.83
733	13.99	202.31	-0.87
734	13.19	201.28	-0.88
735	4.51	199.63	-0.3[illegible]
736	9.03	200.21	-0.72
737	11.16	199.46	-0.87
738	13.64	198.59	-0.94
739	13.51	193.04	-1.13
740	12.28	190.83	-1.19
741	23.89	201.68	-1.05
742	27.52	200.49	-1.14
743	20.72	197.12	-1.12
744	20.79	195.01	-1.20
745	20.62	190.50	-1.34
746	17.44	190.98	-1.27
747	15.43	190.29	-1.26
750	11.82	181.40	-1.36
751	20.89	185.44	-1.35
752	20.93	181.01	-1.41
753	3.38	178.40	-0.20
754	1.99	178.19	0.01
755	2.73	172.41	0.21
756	13.58	177.97	-1.32
757	13.33	175.83	-1.26
758	17.88	182.77	-1.32
759	15.11	181.51	-1.31
760	20.64	178.51	-1.38
761	20.74	176.98	-1.43
762	19.98	174.74	-1.57
763	22.51	181.13	-1.35
764	24.78	181.20	-1.35
765	26.70	182.51	-1.37
766	28.04	180.42	-1.44
769	12.82	169.42	-0.98

Table 6 (continued)

Point	Latitude ($\phi'°$)	W.Longitude ($\lambda°$)	Elevation (km)
771	5.47	163.42	-0.11
772	6.67	163.08	-0.24
773	10.09	152.57	0.07
774	4.98	152.81	0.64
775	7.69	145.45	1.39
785	7.63	174.88	-0.62
786	6.46	173.22	-0.40
787	6.51	177.11	-0.58
788	11.03	175.32	-1.09
791	9.47	169.30	-0.62
792	7.57	171.73	-0.47
793	16.02	170.53	-1.30
796	6.87	168.43	-0.26
797	8.94	157.60	-0.22
798	11.89	170.26	0.09
800	-26.32	9.19	2.27
801	-26.90	7.60	2.29
802	-24.35	5.98	2.43
803	-27.04	14.72	2.21
804	-23.96	14.97	2.13
806	-18.50	4.55	2.45
807	-17.05	8.30	2.35
808	-23.96	7.71	2.42
809	-23.06	7.45	2.46
810	-22.96	4.33	2.50
811	-21.25	5.54	2.55
812	-22.66	6.17	2.49
813	-19.10	1.23	2.49
814	-17.64	3.49	2.39
815	-13.97	3.11	2.10
817	-12.45	1.08	1.99
818	-14.99	358.73	2.32
819	-8.64	2.44	1.70
820	-9.62	0.57	1.78
822	-10.65	356.06	2.30
823	-7.61	358.32	1.80
824	-14.26	6.71	2.13
825	-4.60	0.52	1.40
826	-4.20	2.41	1.36
827	-5.35	358.71	1.60
828	-3.72	358.26	1.51
829	-8.58	4.97	1.69
830	-10.67	11.58	1.71
831	-10.39	10.20	1.80

Table 6 (continued)

Point	Latitude (ϕ'°)	W.Longitude (λ°)	Elevation (km)
832	-8.92	10.47	1.66
833	-6.88	13.95	1.29
834	-5.05	9.45	1.39
835	-4.28	9.40	1.35
836	-3.22	12.19	1.20
837	1.40	8.21	0.89
839	-12.46	14.81	1.58
840	-16.75	13.34	1.98
841	-16.26	12.42	2.03
842	-14.10	11.75	1.94
843	-15.30	13.36	1.88
844	-18.90	9.24	2.50
845	-13.14	9.96	2.03
846	-8.83	7.30	1.70
847	-22.41	10.54	2.42
848	-18.66	12.07	2.24
849	-18.28	14.43	1.97
850	-23.11	13.91	2.17
851	-17.76	16.08	1.77
852	-22.63	16.42	2.00
853	-22.36	15.28	2.07
854	-20.35	14.52	2.09
856	-21.74	10.28	2.47
857	-23.56	16.12	2.06
858	-22.64	17.44	1.92
859	-21.42	19.60	1.65
861	-25.49	16.83	2.13
862	-24.17	2.73	2.50
863	-22.07	0.23	2.56
864	-21.52	355.78	3.06
865	-20.33	359.84	2.57
866	-17.61	358.86	2.50
867	-14.93	357.97	2.41
868	-16.70	353.81	3.08
869	-12.60	356.03	2.47
870	-11.91	351.71	2.93
871	-11.14	353.80	2.62
872	-9.71	356.39	2.19
873	-5.13	355.32	1.95
874	-9.01	354.63	2.35
875	-5.84	353.08	2.26
876	-6.39	352.13	2.42
877	-1.95	350.11	2.27
878	-2.31	352.17	2.08

Table 6 (continued)

Point	Latitude (ϕ'°)	W.Longitude (λ°)	Elevation (km)
879	-0.53	353.51	1.78
880	3.37	348.53	1.96
881	4.09	354.69	1.27
882	-26.00	358.09	2.71
883	-24.09	358.91	2.65
884	-23.20	356.45	2.93
885	-24.95	358.05	2.73
887	-20.27	353.09	3.46
888	-24.48	354.33	3.11
890	-18.55	355.26	3.05
891	-17.86	353.14	3.27
892	-19.26	351.88	3.55
893	-13.97	352.71	2.98
895	-15.16	349.05	3.48
896	-8.74	350.94	2.75
897	-9.99	352.55	2.66
898	-10.40	346.94	3.15
899	-9.21	348.58	2.98
900	-5.87	349.91	2.62
901	-8.50	347.46	2.98
902	-9.18	344.92	3.14
903	-8.33	343.82	3.15
904	-7.54	345.45	3.01
905	-4.51	340.87	3.09
906	-3.69	342.71	2.95
907	-2.55	344.00	2.76
908	-17.21	351.23	3.45
909	-17.75	348.44	3.74
910	-21.95	351.09	3.60
911	-23.85	11.93	2.29
912	-4.13	348.82	2.55
913	2.75	345.33	2.31
914	1.68	344.54	2.46
915	2.24	340.70	2.76
916	0.87	340.30	2.86
917	6.41	342.67	2.35
918	5.26	339.96	2.69
919	5.21	337.72	2.73
920	-24.56	195.70	3.35
921	-25.30	188.66	3.15
922	-28.62	190.66	3.29
923	-22.64	194.05	3.24
924	-2.70	178.67	0.46
925	-2.33	177.80	0.48

Table 6 (continued)

Point	Latitude ($\phi'°$)	W.Longitude ($\lambda°$)	Elevation (km)
926	-3.76	175.30	0.79
927	-7.22	175.06	1.21
928	-5.38	175.55	0.95
929	-9.59	178.31	1.19
930	-10.32	178.34	1.28
931	-10.90	176.26	1.53
932	-9.52	175.94	1.39
933	-10.90	174.25	1.70
934	-9.54	173.45	1.60
935	-11.40	172.77	1.89
936	-14.63	173.92	2.23
937	-15.42	174.38	2.30
938	-11.87	180.08	1.44
939	-12.72	178.20	1.62
940	-13.87	177.27	1.86
941	-14.44	178.01	1.88
942	-15.46	178.27	2.00
946	-15.87	183.61	2.25
947	-16.85	180.85	2.19
948	-17.71	178.81	2.28
949	-16.43	184.88	2.41
950	-17.51	185.68	2.61
951	-18.84	184.16	2.68
952	-19.22	186.27	2.86
954	-20.33	185.76	2.96
955	-21.57	183.31	2.80
956	-17.30	188.29	2.76
957	-22.04	184.28	2.87
958	-22.90	186.08	2.99
959	-22.31	187.74	3.09
960	-24.18	187.47	3.07
961	-24.13	188.68	3.15
962	-21.88	190.41	3.20
963	-18.14	180.18	2.33
964	-19.85	180.49	2.59
965	-19.51	181.73	2.62
966	-21.24	180.31	2.61
969	-22.57	190.55	3.20
970	-24.47	190.96	3.24
971	-23.87	194.09	3.29
972	-25.91	193.19	3.33
973	-17.85	189.05	2.87
974	-18.43	188.36	2.90
975	-19.69	189.22	3.11

Table 6 (continued)

Point	Latitude ($\phi'°$)	W.Longitude ($\lambda°$)	Elevation (km)
976	-19.41	191.38	3.08
977	-12.81	186.94	2.10
978	-14.12	186.69	2.25
979	-14.26	188.49	2.40
980	-15.22	187.60	2.46
981	-15.90	189.42	2.66
982	-16.83	188.38	2.71
988	-19.74	194.56	3.11
989	-21.40	191.82	3.20
991	-15.96	191.33	2.68
992	-16.79	189.47	2.78
993	-11.88	188.48	2.11
994	-7.82	184.97	1.21
995	-2.95	186.49	0.38
996	-3.02	185.52	0.39
997	-7.45	184.34	1.11
1000	-5.31	185.45	0.79
1001	-4.76	183.37	0.67
1002	-6.41	183.39	0.92
1003	-5.35	179.70	0.67
1004	-24.04	139.44	4.36
1005	-25.20	145.86	4.16
1006	-25.09	143.23	4.22
1007	-23.57	143.09	4.23
1008	-21.10	140.33	4.44
1009	-20.85	138.44	4.70
1010	-23.19	140.81	4.33
1011	-25.72	140.52	4.25
1012	-18.64	138.66	4.70
1013	-19.78	140.37	4.45
1014	-15.92	141.27	4.31
1015	-16.77	137.86	4.83
1016	-15.65	136.83	5.05
1017	-13.58	136.48	5.10
1018	-13.18	137.76	4.87
1019	-14.66	133.00	5.73
1020	-14.23	131.82	5.95
1021	-13.42	129.95	6.30
1022	-10.87	131.73	5.91
1023	-10.30	132.20	5.81
1024	-12.23	130.61	6.15
1025	-30.70	143.11	4.19
1026	-31.97	147.55	4.03
1027	-27.84	150.44	4.11

Table 6 (continued)

Point	Latitude ($\phi'°$)	W.Longitude ($\lambda°$)	Elevation (km)
1028	-14.48	129.26	6.43
1029	-15.36	129.36	6.43
1030	-13.47	127.51	6.66
1031	-14.27	125.40	7.02
1032	-13.18	126.57	6.78
1033	-10.81	128.19	6.47
1034	-10.57	126.85	6.65
1035	-10.00	122.96	7.11
1036	-8.52	125.99	6.62
1037	-7.39	123.86	6.77
1038	-8.07	123.83	6.84
1039	-17.73	177.95	2.34
1040	-19.38	177.28	2.63
1041	-9.83	121.36	7.32
1042	-6.75	121.50	7.00
1043	-6.95	120.01	7.19
1044	-4.93	121.73	6.79
1045	-4.23	123.45	6.51
1046	-2.90	126.26	6.04
1047	1.06	120.90	6.26
1048	-2.32	120.39	6.67
1049	2.18	122.66	5.95
1050	5.76	123.40	5.53
1051	3.94	119.11	6.14
1052	4.42	116.56	6.34
1053	1.39	124.66	5.81
1054	-15.46	132.98	5.75
1056	-14.74	131.83	5.95
1200	32.89	89.14	2.54
1201	32.16	96.14	2.82
1202	32.46	86.92	2.61
1203	34.05	81.76	2.48
1204	38.90	83.81	1.87
1205	39.67	80.20	1.83
1206	40.35	75.62	1.22
1207	42.19	89.47	1.46
1208	42.19	82.59	1.57
1209	44.10	78.73	1.25
1210	43.69	74.82	0.78
1211	40.84	69.58	0.33
1212	49.08	68.77	-0.39
1213	47.49	73.48	0.22
1215	27.20	76.66	2.61
1216	33.31	76.25	1.98

Table 6 (continued)

Point	Latitude ($\phi'°$)	W.Longitude ($\lambda°$)	Elevation (km)
1217	32.77	72.61	1.43
1218	37.46	70.64	0.69
1219	39.47	66.17	0.20
1220	41.48	64.64	-0.05
1221	44.56	64.04	-0.31
1222	45.57	69.87	-0.05
1223	44.24	53.16	-0.90
1224	40.55	56.87	-0.43
1225	37.64	56.36	-0.21
1226	39.30	41.99	-1.33
1227	41.55	50.92	-0.78
1228	39.17	46.51	-0.91
1229	33.98	66.34	0.61
1230	32.16	67.06	0.81
1231	25.98	67.84	1.71
1232	27.00	55.94	0.69
1233	28.00	57.63	0.66
1234	28.80	59.45	0.60
1235	25.28	53.93	0.72
1236	32.33	56.59	0.20
1237	34.52	56.59	0.03
1238	34.27	52.16	-0.05
1239	33.40	50.48	-0.00
1240	32.35	48.58	-0.07
1241	27.38	50.26	0.38
1242	26.32	43.25	-0.24
1243	27.07	40.16	-0.60
1244	30.07	51.17	0.31
1245	33.92	46.32	-0.46
1246	33.23	43.65	-0.70
1247	34.29	42.98	-0.85
1248	32.47	41.05	-0.94
1249	32.02	38.93	-1.09
1250	36.33	43.90	-0.91
1251	41.94	42.18	-1.49
1252	38.52	35.03	-1.61
1253	40.90	34.54	-1.74
1254	37.40	39.59	-1.41
1255	25.94	37.77	-0.64
1256	26.12	35.29	-0.80
1257	29.39	39.83	-0.86
1258	33.75	30.38	-1.55
1259	34.01	34.25	-1.40
1260	41.12	24.57	-1.70

Table 6 (continued)

Point	Latitude ($\phi'°$)	W.Longitude ($\lambda°$)	Elevation (km)
1261	39.22	25.24	-1.61
1262	26.02	31.88	-1.01
1263	28.84	31.28	-1.26
1264	33.21	21.22	-1.12
1265	34.35	25.70	-1.40
1266	37.83	30.40	-1.71
1267	26.66	24.14	-0.89
1268	30.21	21.92	-0.99
1269	33.07	17.17	-1.06
1270	34.17	11.82	-1.13
1271	38.15	21.24	-1.40
1272	38.84	18.49	-1.37
1273	43.60	9.10	-1.46
1274	42.61	15.11	-1.56
1275	41.66	10.57	-1.38
1276	39.26	11.76	-1.30
1277	26.48	13.00	-0.75
1278	30.28	14.89	-0.95
1279	28.99	13.21	-0.90
1280	34.09	6.94	-1.05
1281	32.61	2.67	-0.88
1282	36.75	8.66	-1.15
1283	39.96	3.20	-1.17
1284	38.47	356.73	-0.90
1285	42.61	0.45	-1.24
1286	43.20	356.81	-1.05
1287	41.76	355.24	-0.94
1288	26.76	2.87	-0.61
1289	26.14	358.00	-0.38
1290	31.09	5.98	-0.92
1291	34.16	0.23	-0.88
1292	32.83	357.69	-0.70
1293	34.16	353.91	-0.57
1294	41.59	350.45	-0.59
1295	40.90	348.44	-0.57
1296	26.94	355.44	-0.27
1297	26.55	349.91	0.11
1298	31.91	354.98	-0.50
1299	33.12	350.12	-0.31
1300	30.11	355.39	-0.42
1301	31.94	345.26	0.20
1302	35.16	352.61	-0.60
1303	40.40	343.72	-0.11
1304	38.82	338.63	0.37

Table 6 (continued)

Point	Latitude ($\phi'°$)	W.Longitude ($\lambda°$)	Elevation (km)
1305	38.90	346.66	-0.31
1306	45.03	347.46	-0.46
1307	45.56	341.72	-0.44
1308	29.25	346.92	0.21
1309	32.90	340.80	0.55
1310	36.54	343.38	0.14
1311	40.86	334.43	0.31
1312	46.02	334.69	-0.21
1313	25.37	332.09	1.46
1314	31.31	337.64	0.81
1315	34.05	337.95	0.64
1316	32.51	333.39	0.88
1317	33.77	329.42	0.88
1318	35.27	332.58	0.75
1319	38.48	331.39	0.54
1320	41.57	327.64	0.24
1321	39.70	321.12	0.11
1322	48.85	330.63	-0.20
1323	40.65	324.47	0.18
1327	32.44	324.88	0.76
1328	33.16	317.35	0.47
1329	34.29	322.89	0.64
1330	36.06	323.51	0.40
1331	39.88	315.79	0.10
1332	40.30	310.02	0.21
1333	47.50	319.22	-0.39
1334	45.02	320.30	-0.24
1335	26.60	315.09	0.89
1339	33.93	308.22	0.41
1340	37.47	311.21	0.28
1341	39.74	306.46	0.19
1342	44.12	306.68	-0.15
1343	48.36	306.27	-0.51
1344	28.10	305.75	0.82
1345	27.67	309.66	0.68
1346	30.75	309.23	0.50
1347	33.05	303.63	0.57
1348	33.39	298.94	0.64
1351	41.97	298.98	-0.06
1352	40.04	297.66	0.12
1353	39.11	292.77	0.21
1354	44.71	295.85	-0.26
1355	45.42	302.47	-0.30
1356	29.07	300.75	0.96

Table 6 (continued)

Point	Latitude ($\phi'°$)	W.Longitude ($\lambda°$)	Elevation (km)
1357	30.75	298.49	0.86
1358	33.98	292.80	0.62
1359	33.15	288.43	0.66
1360	38.15	295.77	0.28
1361	35.48	292.40	0.52
1362	41.46	294.60	0.01
1363	27.07	292.35	1.16
1364	41.56	287.23	-0.05
1365	39.55	289.24	0.17
1367	36.58	288.41	0.39
1368	34.58	284.47	0.44
1369	38.26	284.31	0.13
1371	40.31	273.00	0.42
1372	28.11	276.51	1.28
1373	25.77	272.22	-0.11
1374	21.93	272.64	-0.06
1375	33.87	275.91	0.76
1376	33.50	278.92	0.50
1377	32.58	273.36	1.11
1378	41.81	272.25	0.35
1379	36.95	278.36	0.25
1380	28.88	266.78	1.60
1381	25.96	266.99	1.69
1382	28.76	262.28	1.50
1383	29.76	271.04	1.56
1384	33.38	266.60	1.21
1385	34.10	262.07	0.90
1386	37.14	268.04	0.85
1387	36.86	264.27	0.64
1388	40.58	261.42	-0.07
1389	39.69	254.63	-0.41
1390	38.74	260.81	0.11
1391	38.52	256.11	-0.18
1392	30.11	263.78	1.46
1393	32.80	257.38	0.73
1394	33.00	252.65	0.23
1395	36.26	260.43	0.46
1397	28.55	253.49	0.79
1399	32.60	248.76	0.06
1400	32.85	243.68	-0.20
1401	34.43	250.44	-0.04
1402	36.57	252.28	-0.15
1403	36.71	249.38	-0.35
1404	39.31	243.83	-0.65

Table 6 (continued)

Point	Latitude (ϕ'°)	W.Longitude (λ°)	Elevation (km)
1405	42.84	246.10	-0.88
1406	40.44	238.37	-0.83
1407	28.16	243.36	0.15
1408	29.83	243.52	0.00
1409	34.37	238.77	-0.47
1410	33.21	233.16	-0.52
1411	36.62	238.40	-0.62
1412	38.61	236.81	-0.76
1413	41.76	233.28	-1.06
1414	40.16	227.87	-1.09
1415	24.71	235.57	0.08
1418	34.23	230.68	-0.62
1419	34.33	226.31	-0.86
1420	32.47	223.79	-0.94
1421	38.20	226.78	-1.05
1422	41.53	223.92	-1.38
1423	40.85	218.56	-1.48
1424	30.24	226.66	-0.67
1425	26.33	226.48	-0.53
1426	33.67	221.08	-1.22
1427	32.09	216.41	-1.07
1428	36.60	221.96	-1.28
1429	41.47	209.25	-1.29
1431	28.76	215.29	-0.97
1432	25.24	218.28	-0.94
1433	29.84	217.03	-1.03
1434	33.63	210.06	-0.94
1435	32.77	205.26	-1.08
1436	34.48	215.74	-1.13
1437	36.45	210.24	-1.11
1438	39.11	204.75	-1.27
1439	41.34	199.88	-1.65
1440	44.50	207.00	-1.45
1441	29.06	210.45	-0.86
1442	32.44	208.58	-0.95
1443	29.86	205.87	-0.99
1444	31.98	202.13	-1.18
1445	33.82	196.44	-1.37
1446	33.71	202.69	-1.21
1447	36.98	204.67	-1.22
1448	37.86	201.07	-1.38
1449	41.25	196.44	-1.51
1450	39.59	194.01	-1.47
1451	25.55	197.21	-1.21

Table 6 (continued)

Point	Latitude (ϕ'°)	W.Longitude (λ°)	Elevation (km)
1452	27.17	194.91	-1.31
1454	34.34	193.01	-1.42
1455	34.64	188.12	-1.44
1456	36.35	193.82	-1.45
1457	40.74	190.63	-1.45
1458	38.48	187.50	-1.46
1459	38.74	182.23	-1.44
1460	47.28	190.71	-1.66
1461	49.44	193.51	-1.72
1462	51.40	189.44	-1.79
1465	34.84	184.48	-1.40
1466	34.18	179.09	-1.37
1467	37.50	179.52	-1.45
1468	40.60	172.75	-1.69
1469	47.42	180.58	-1.60
1470	45.12	180.24	-1.54
1471	27.17	176.76	-1.44
1472	26.83	174.36	-1.51
1473	27.91	178.59	-1.38
1476	33.63	174.03	-1.53
1477	32.74	170.48	-1.63
1478	34.98	176.50	-1.46
1479	36.70	173.83	-1.64
1480	38.77	170.96	-1.74
1481	44.25	172.64	-1.80
1482	39.59	165.40	-1.81
1486	42.76	163.94	-1.84
1487	44.83	157.08	-1.62
1489	39.66	158.53	-1.68
1490	49.65	151.72	-1.61
1491	44.14	147.81	-1.17
1492	45.06	149.70	-1.16
1493	40.78	145.44	-1.14
1494	43.88	138.75	-1.33
1496	50.83	140.36	-1.52
1497	47.85	138.94	-1.38
1498	46.87	129.56	-0.01
1499	43.72	134.23	-0.45
1500	39.51	132.99	0.06
1501	38.71	130.83	0.60
1502	39.10	136.40	-0.62
1503	38.24	127.05	1.18
1504	40.99	128.36	0.77
1505	34.71	131.29	0.98

Table 6 (continued)

Point	Latitude ($\phi'°$)	W.Longitude ($\lambda°$)	Elevation (km)
1506	32.21	129.53	1.45
1507	33.79	126.71	1.76
1508	28.70	125.77	2.56
1509	26.96	122.74	3.26
1510	27.04	126.25	2.77
1511	26.49	124.37	3.11
1512	33.26	123.02	2.41
1513	39.55	121.35	1.70
1514	42.68	119.97	1.41
1515	45.41	123.65	0.72
1516	47.03	120.99	0.70
1517	46.21	115.13	0.95
1519	27.07	118.79	3.68
1520	25.77	116.98	3.83
1521	41.14	110.35	1.67
1522	40.07	113.97	1.82
1523	44.41	109.93	1.18
1524	41.43	117.76	1.60
1525	35.91	117.84	2.53
1526	33.38	116.57	3.09
1527	32.64	112.90	3.16
1529	49.45	116.20	0.46
1530	48.17	112.08	0.70
1531	55.05	114.73	-0.30
1532	28.58	116.03	3.67
1533	30.00	113.75	3.50
1534	26.49	109.24	3.90
1535	25.60	104.79	3.84
1536	32.91	107.86	3.01
1537	32.60	104.43	2.95
1538	37.51	111.12	2.20
1539	35.22	108.70	2.81
1540	39.93	105.43	1.85
1541	39.37	101.64	1.85
1542	42.79	106.90	1.46
1543	45.01	100.83	1.06
1544	48.36	96.13	0.61
1545	27.70	106.12	3.63
1546	31.37	99.75	2.97
1547	33.81	99.78	2.62
1548	36.38	98.95	2.24
1549	37.52	102.84	2.13
1550	42.40	97.76	1.43
1551	40.14	94.12	1.73

Table 6 (continued)

Point	Latitude ($\phi'°$)	W.Longitude ($\lambda°$)	Elevation (km)
1552	38.21	95.84	1.94
1553	44.49	91.01	1.18
1554	54.27	97.24	-0.16
1555	51.92	90.92	0.22
1556	58.69	102.97	-0.68
1557	58.77	94.70	-0.74
1558	35.59	93.58	2.25
1559	38.86	89.10	1.81
1561	28.97	94.98	3.16
1562	43.27	85.11	1.40
1564	51.87	125.59	-0.14
1565	66.41	278.19	-1.28
1566	55.18	93.24	-0.26
1568	64.53	109.29	-0.95
1569	54.85	88.15	-0.16
1570	59.11	115.38	-0.88
1571	52.41	297.19	-0.83
1573	58.83	289.51	-1.30
1574	62.09	289.20	-1.30
1577	45.07	278.84	-0.32
1578	43.20	244.44	-0.93
1579	49.21	241.31	-1.51
1580	41.48	236.00	-0.97
1581	55.27	227.01	-1.80
1582	50.64	225.67	-1.91
1583	59.63	222.11	-1.82
1584	66.61	216.34	-2.28
1586	58.71	214.02	-2.34
1587	53.74	195.93	-1.98
1588	48.93	199.55	-1.80
1591	60.27	207.25	-2.67
1592	79.83	215.38	-1.17
1593	72.21	214.48	-2.15
1594	60.58	230.91	-1.60
1595	55.01	256.17	-1.40
1596	48.77	271.03	0.01
1597	51.88	267.35	-0.50
1598	69.23	270.36	-1.25
1599	50.34	77.03	0.35
1600	11.58	133.75	11.80
1601	14.28	129.47	9.55
1602	15.23	130.85	12.57
1603	17.49	133.52	27.05
1604	17.42	129.33	11.86

Table 6 (continued)

Point	Latitude ($\phi'°$)	W.Longitude ($\lambda°$)	Elevation (km)
1605	14.35	131.49	11.42
1606	19.06	133.10	25.07
1607	23.23	133.50	4.29
1608	20.67	135.44	6.03
1609	18.75	135.79	9.06
1610	53.96	81.20	0.08
1611	50.08	61.27	-0.83
1612	51.95	64.53	-0.86
1613	53.60	70.97	-0.62
1614	49.43	43.77	-1.90
1615	60.68	58.02	-2.15
1616	54.46	39.00	-2.53
1617	49.78	34.72	-2.26
1618	53.94	31.64	-2.63
1619	47.43	28.00	-2.26
1620	50.93	18.40	-2.46
1621	48.07	13.65	-1.98
1622	43.65	23.87	-1.94
1623	62.59	23.87	-2.78
1624	50.20	8.31	-1.85
1625	65.82	21.57	-2.51
1627	76.89	55.11	-1.49
1628	85.03	7.78	-0.43
1629	74.73	13.62	-1.50
1630	72.02	15.64	-1.83
1631	73.74	358.35	-1.49
1632	77.04	334.32	-1.00
1633	73.28	333.42	-1.26
1634	58.77	347.69	-1.74
1635	43.25	5.32	-1.44
1636	50.03	356.91	-1.24
1638	62.27	353.69	-1.34
1639	65.25	329.04	-1.23
1640	61.39	336.11	-1.48
1641	56.56	337.64	-1.36
1642	54.41	333.71	-0.89
1643	49.49	339.20	-1.02
1644	49.59	334.95	-0.68
1645	54.15	188.86	-2.00
1646	54.53	183.15	-1.96
1648	55.00	169.51	-2.27
1649	52.83	160.92	-1.88
1650	57.11	159.09	-1.88
1651	61.06	170.60	-2.40

Table 6 (continued)

Point	Latitude ($\phi'°$)	W.Longitude ($\lambda°$)	Elevation (km)
1652	72.19	306.51	-1.02
1653	60.49	303.50	-1.37
1654	70.17	295.29	-0.55
1655	62.17	318.83	-1.44
1656	68.54	160.89	-2.14
1657	79.01	153.17	-1.02
1658	64.67	139.17	-1.42
1659	60.75	138.32	-1.32
1660	64.88	126.38	-0.97
1661	57.87	134.37	-1.04
1662	53.69	244.57	-1.62
1663	67.21	246.72	-1.39
1666	25.23	191.55	-1.39
1667	26.82	192.22	-1.39
1668	28.62	190.09	-1.49
1669	22.17	190.23	-1.38
1678	78.30	308.32	-0.74

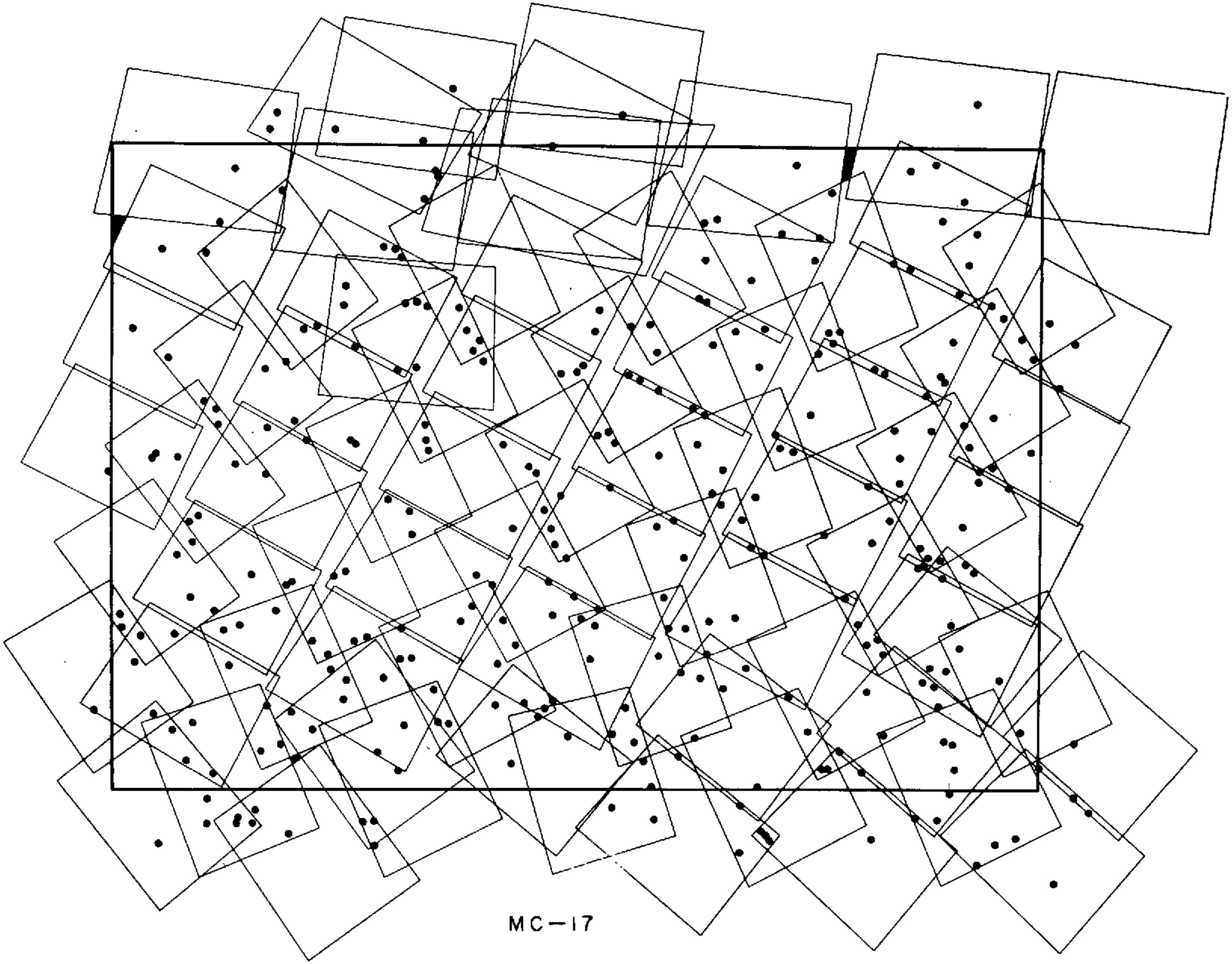

Fig. 1— Sample layout of secondary control net for one Mars chart

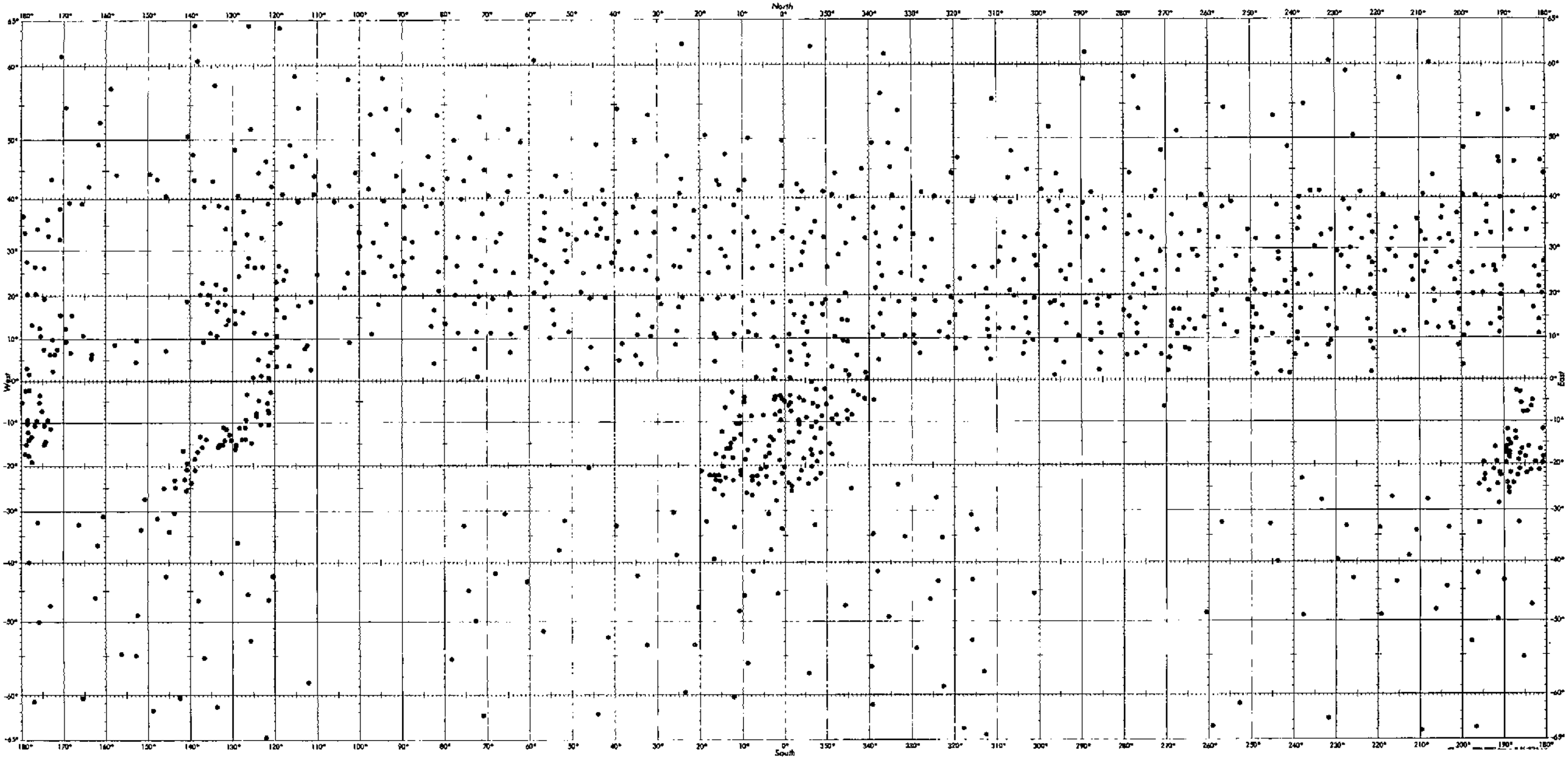

Fig. 2A — The points of the primary control net plotted on a chart of the central latitudes (Mercator projection)

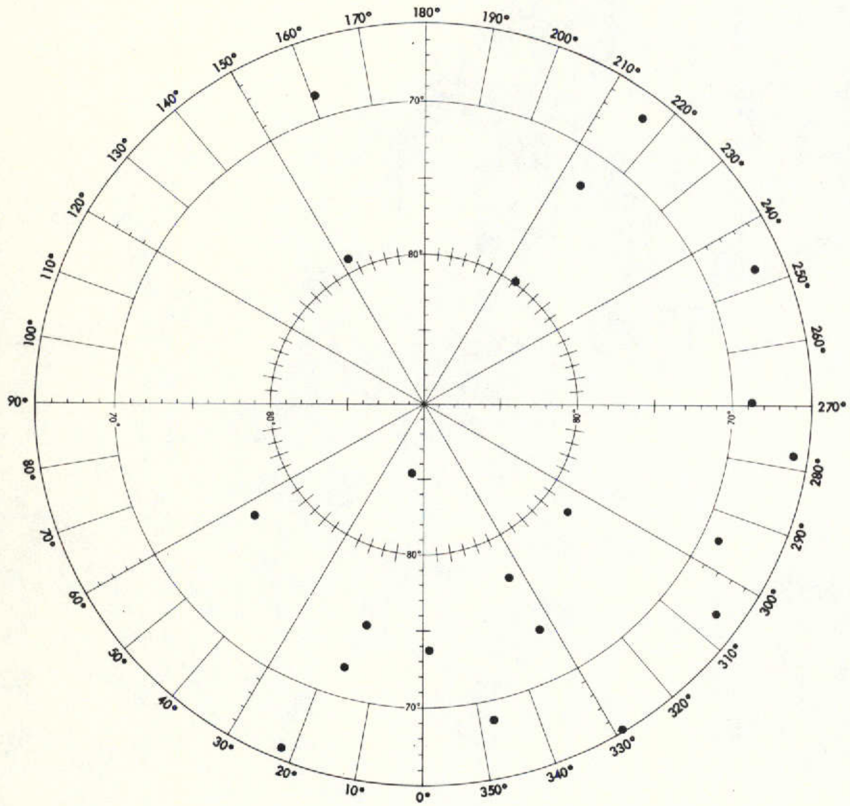

NORTH POLAR REGION

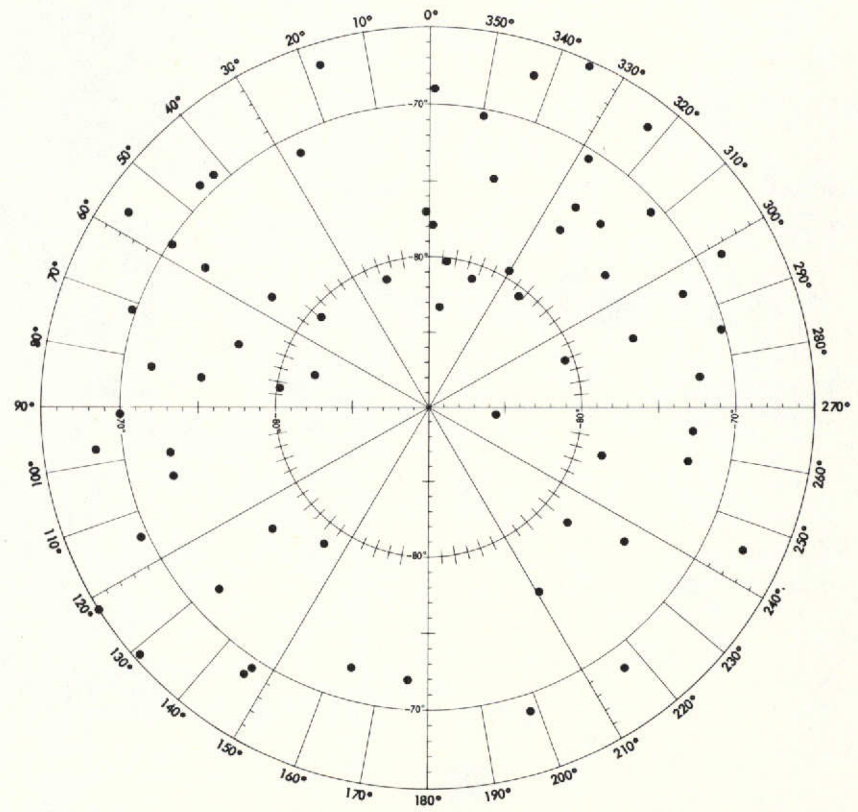

SOUTH POLAR REGION

Fig. 2B — The points of the primary control net plotted on charts of each pole (stereographic projection)

Fig. 3—Control points identified on USGS MC-1 are north of 65° N

Fig. 4—Control points identified on USGS MC-2 are bounded by latitudes 30°N, 65°N and longitudes 120°, 180

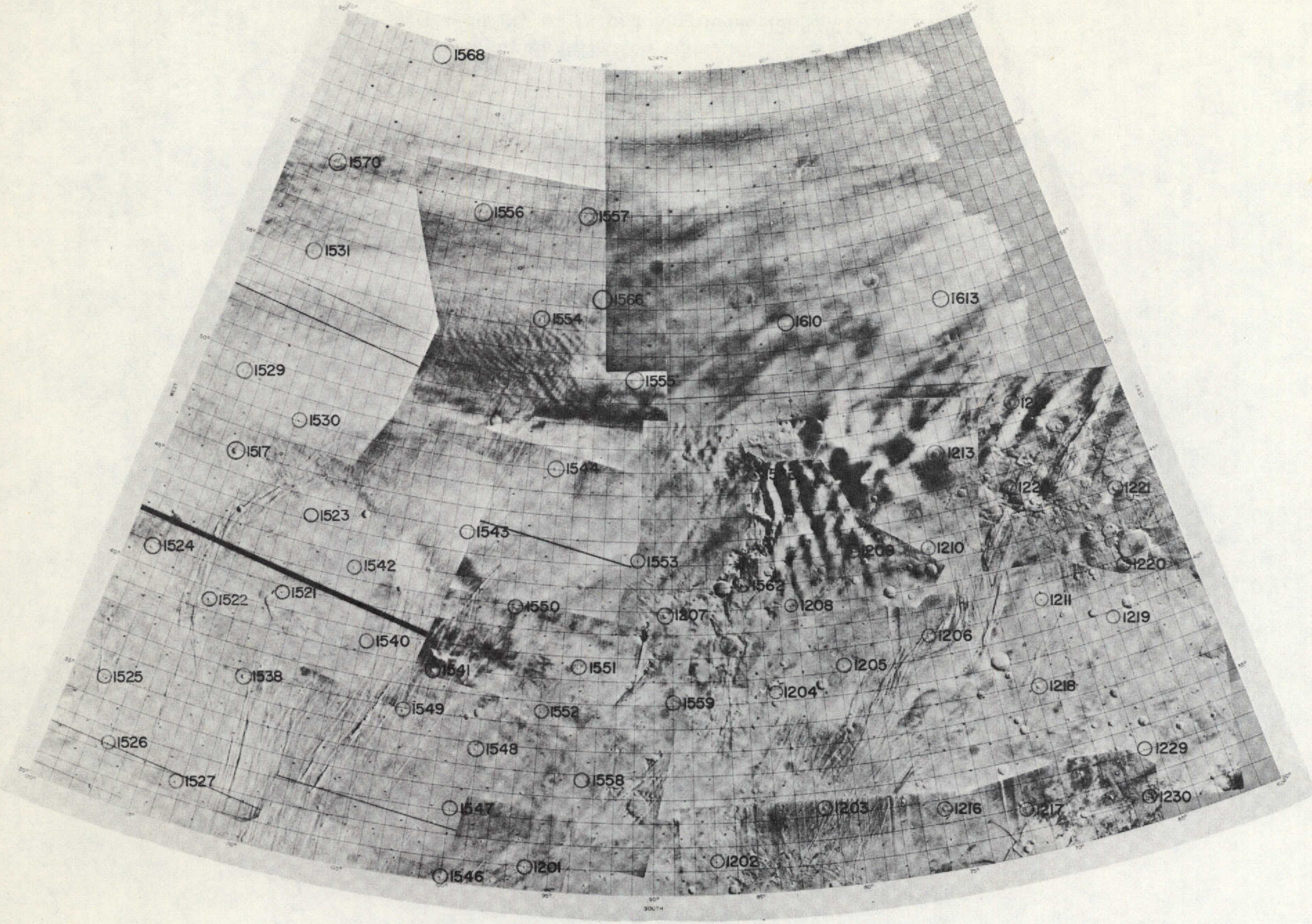

Fig. 5—Control points identified on USGS MC-3 are bounded by latitudes 30°N, 65°N and longitudes 60°, 120°

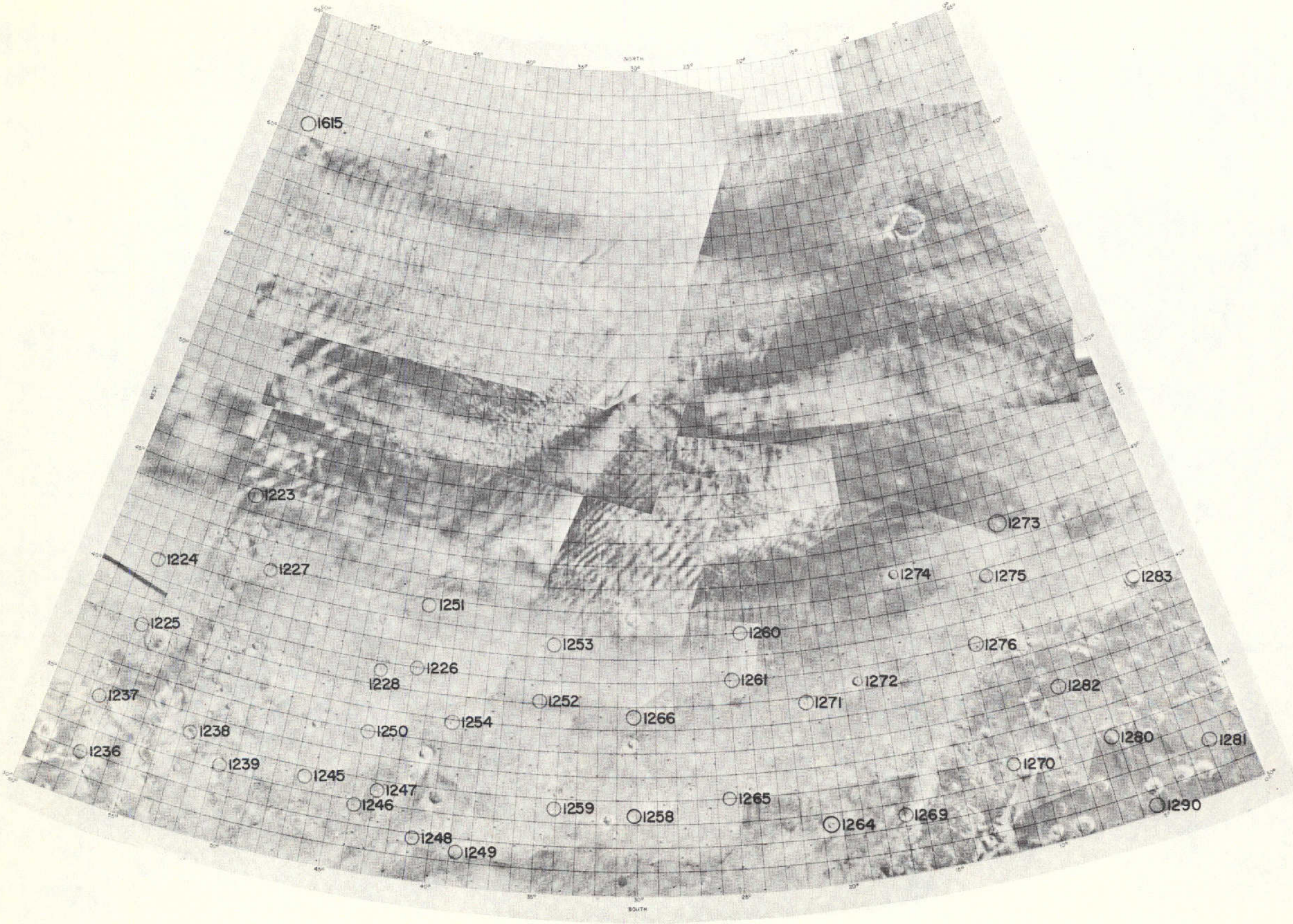

Fig. 6 — Control points identified on USGS MC-4 are bounded by latitudes 30° N, 65° N and longitudes 0°, 60°

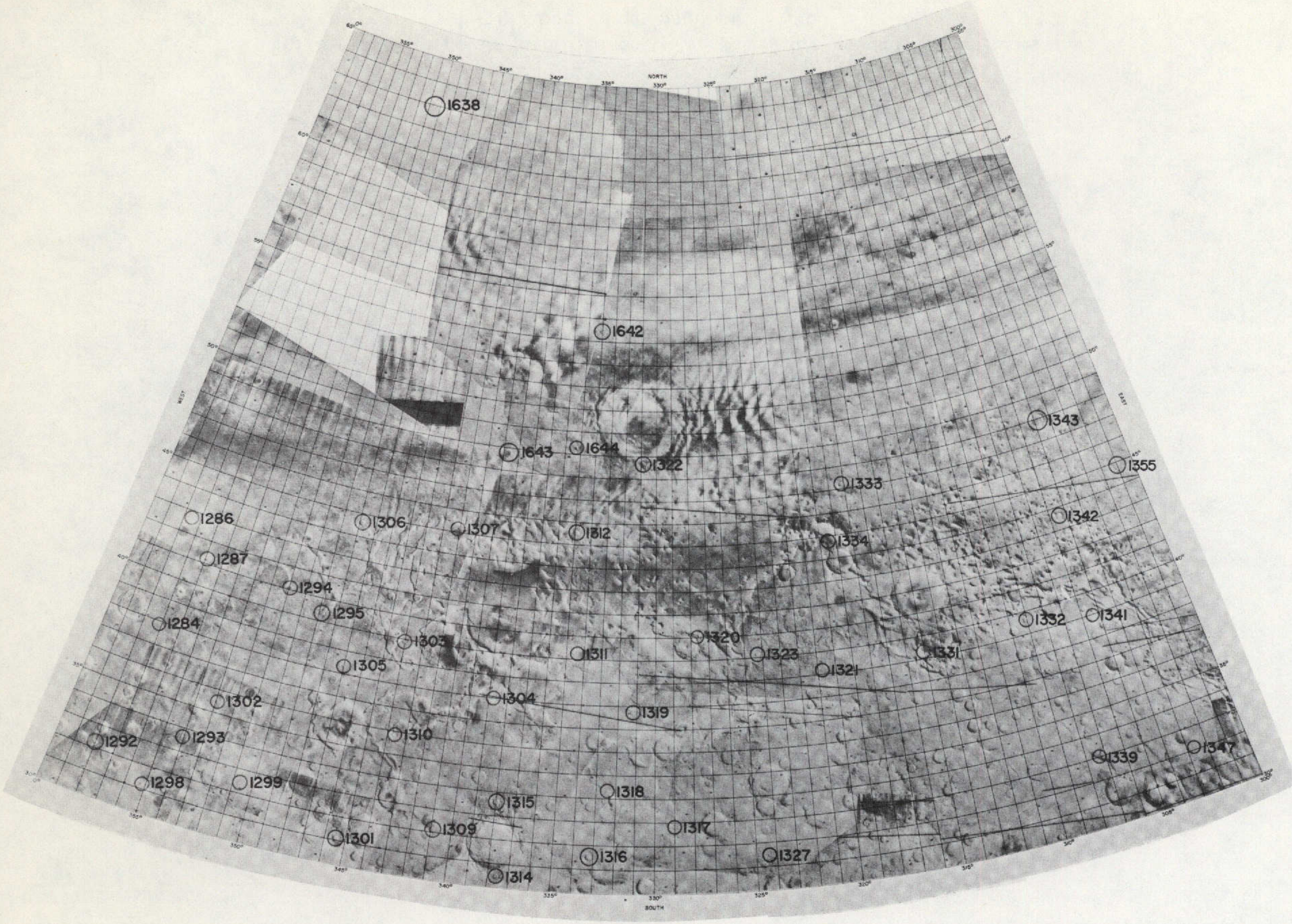

Fig. 7— Control points identified on USGS MC-5 are bounded by latitudes 30° N, 65° N and longitudes 300°, 0°

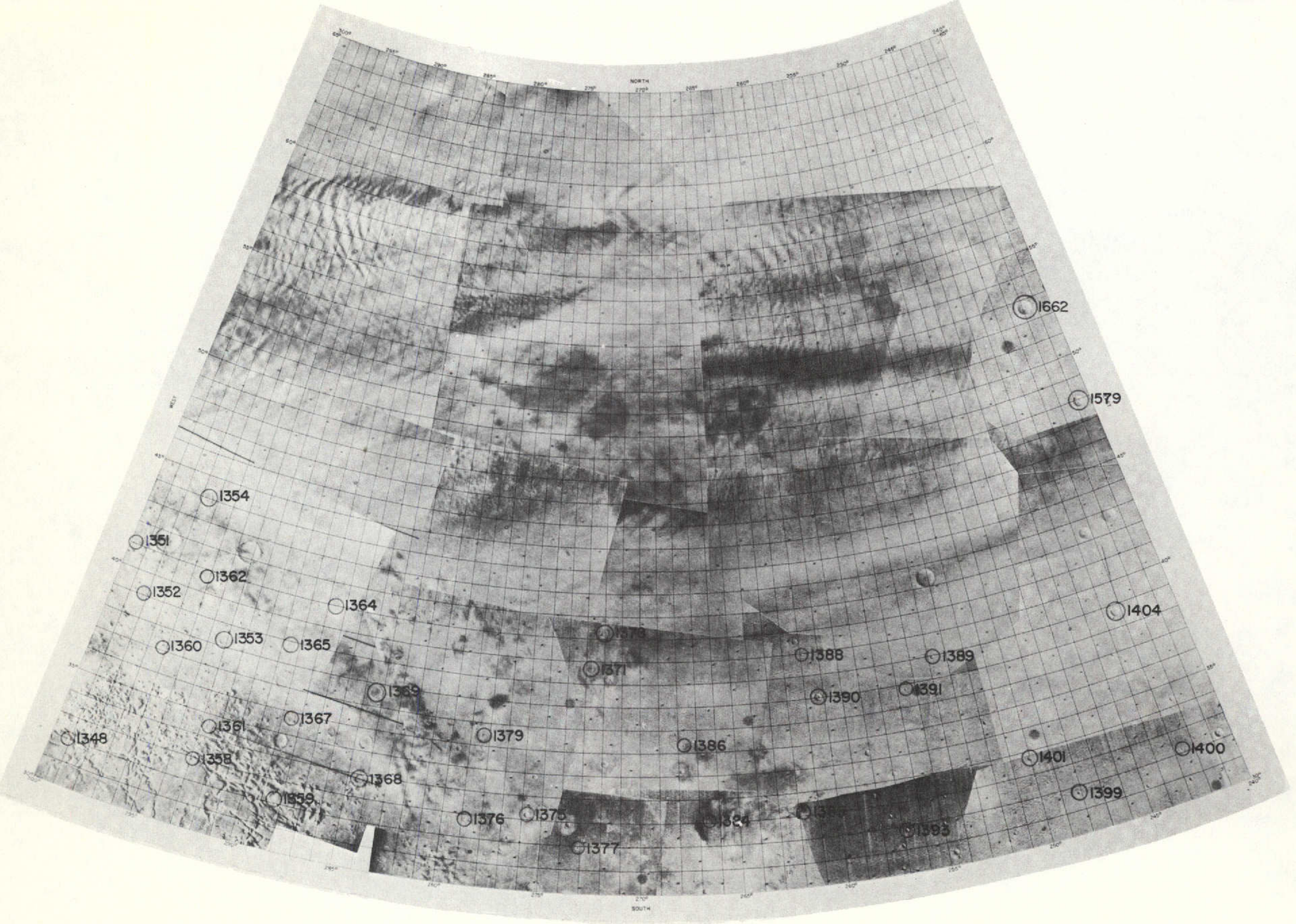

Fig. 8 — Control points identified on USGS MC-6 are bounded by latitudes 30°N, 65°N and longitudes 240°, 300°

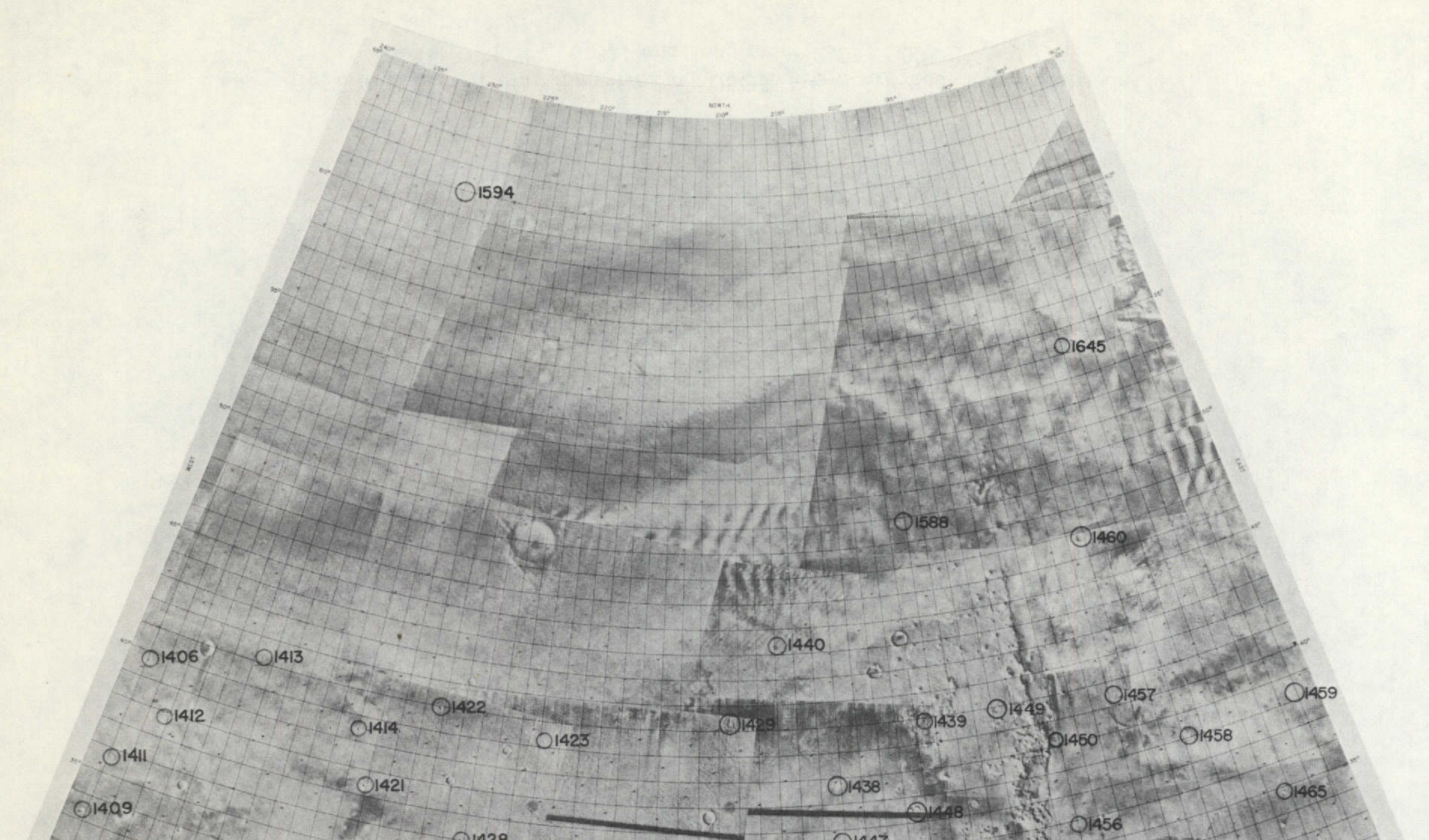

Fig. 9—Control points identified on USGS MC-7 are bounded by latitudes 30°N, 65°N and longitudes 180°, 240°

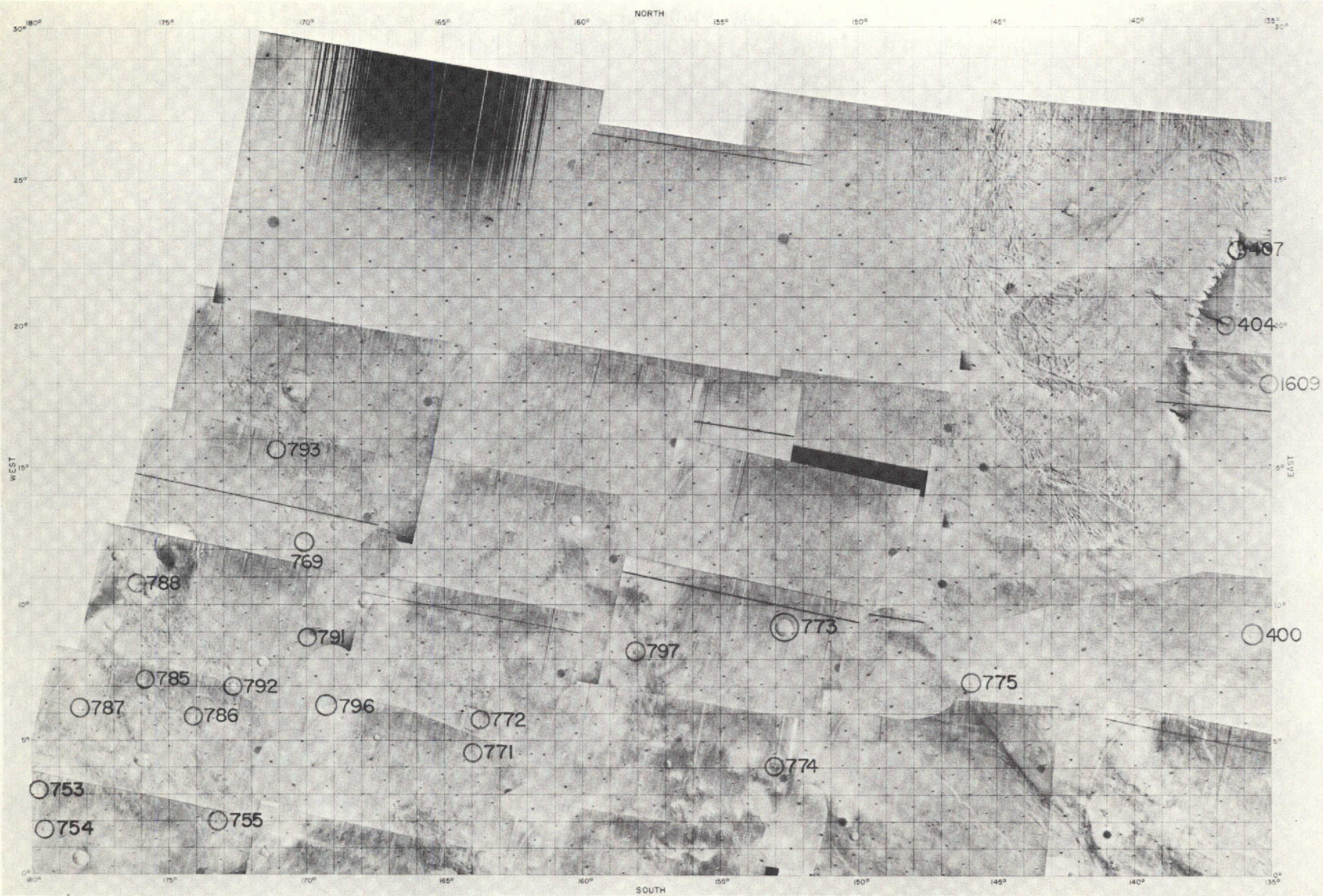

Fig. 10 — Control points identified on USGS MC-8 are bounded by latitudes 0°, 30°N and longitudes 135°, 180°

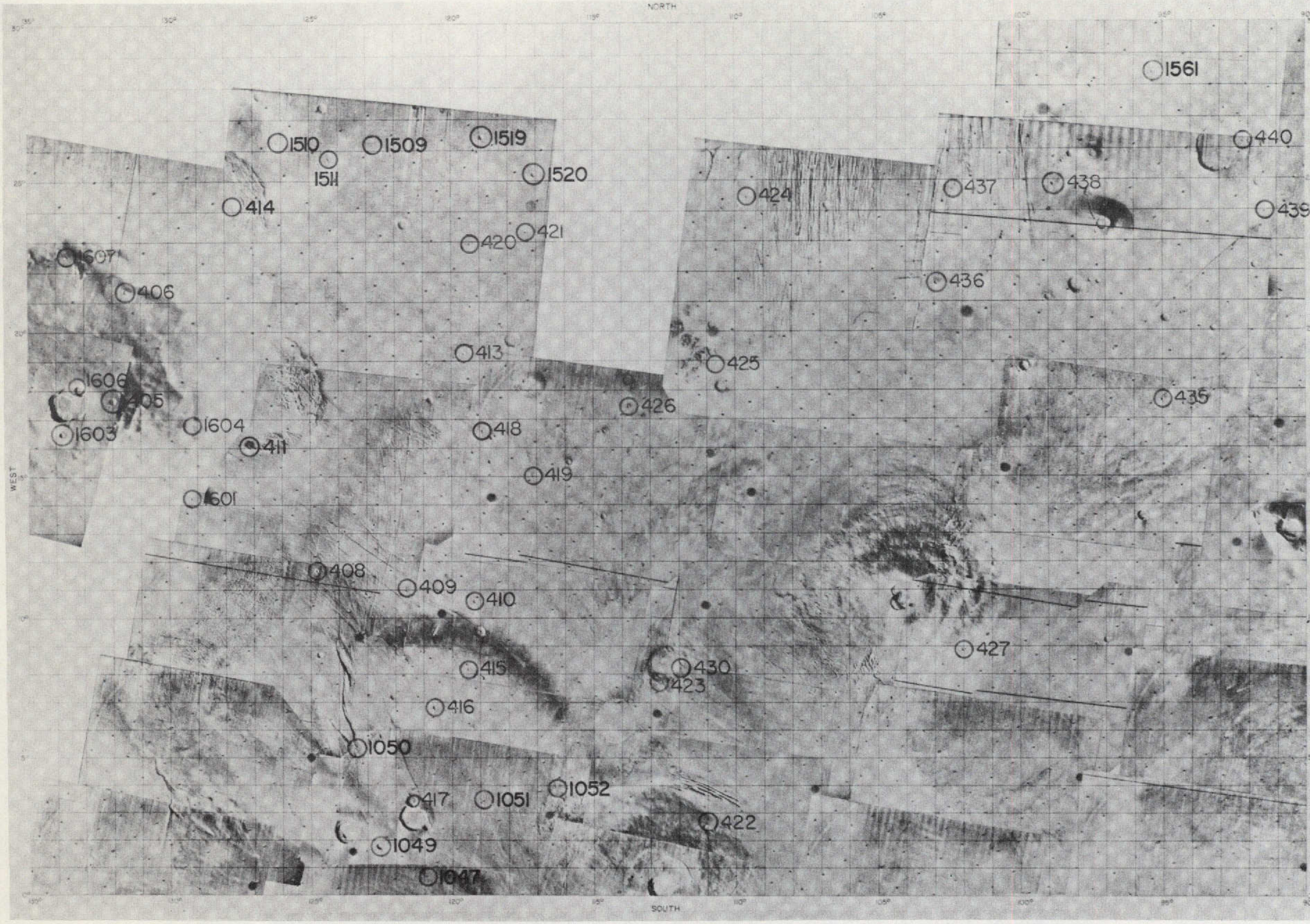

Fig. 11— Control points identified on USGS MC-9 are bounded by latitudes
0°, 30°N and longitudes 90°, 135°

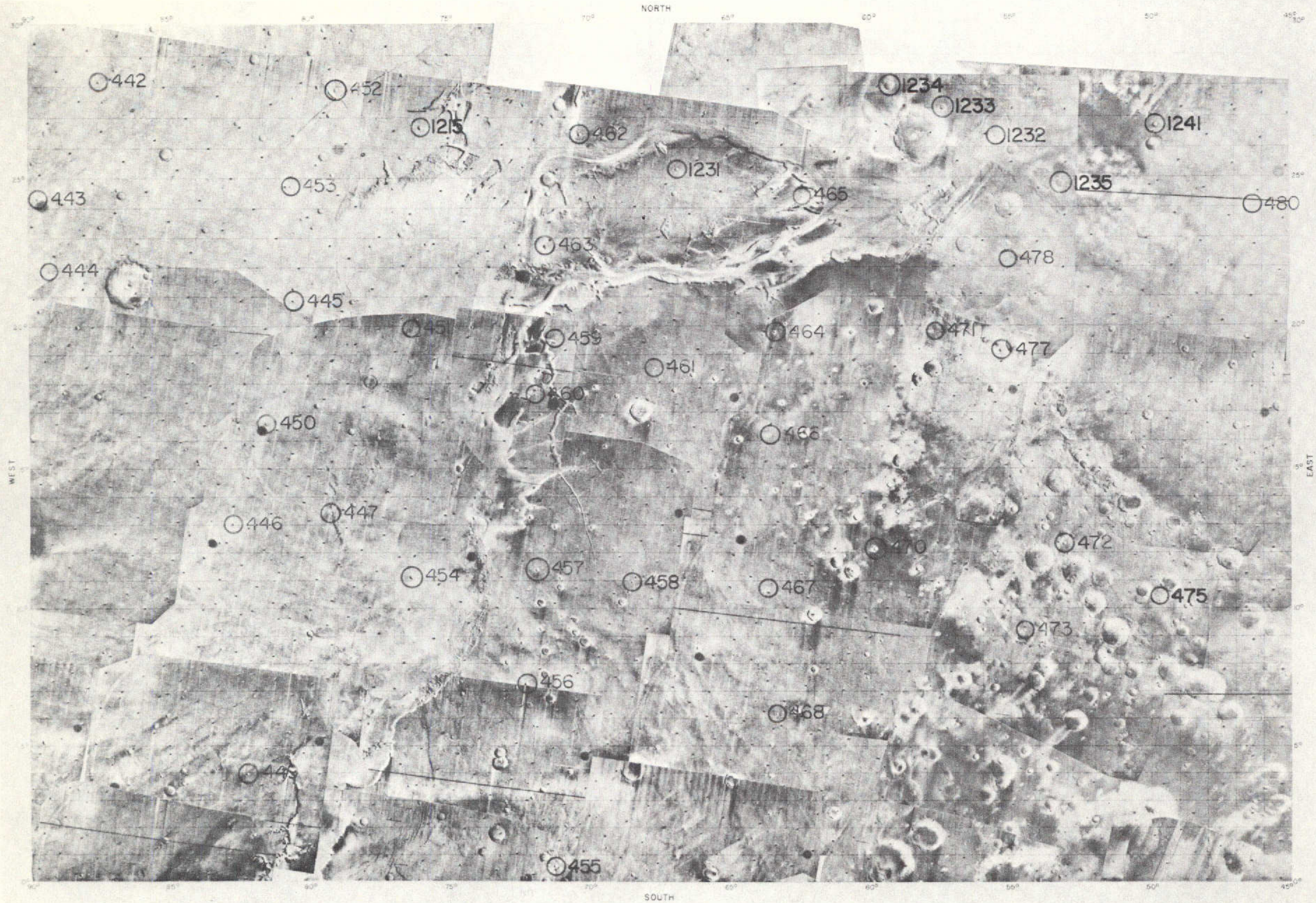

Fig. 12—Control points identified on USGS MC-10 are bounded by latitudes 0°, 30°N and longitudes 45°, 90°

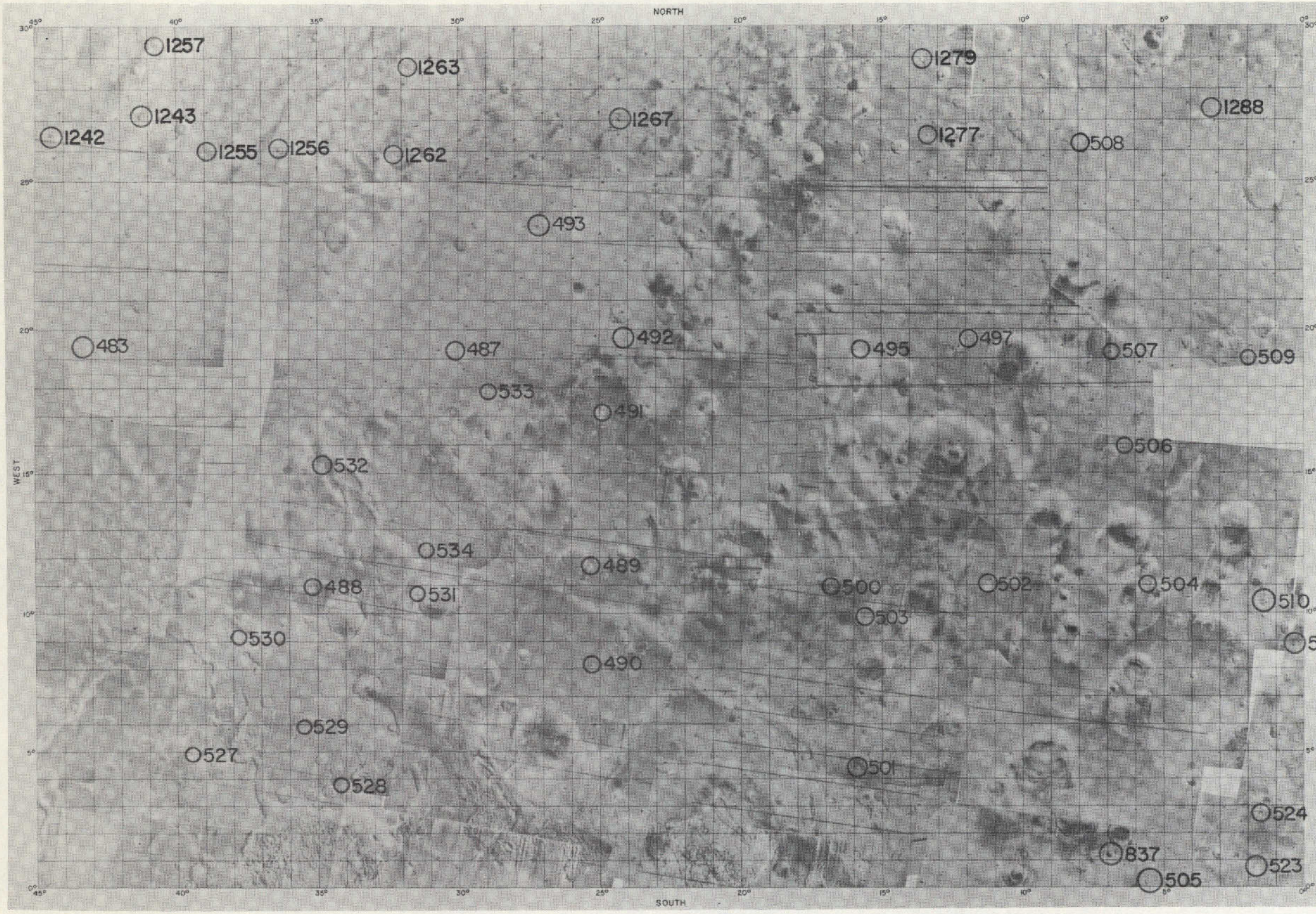

Fig. 13—Control points identified on USGS MC-11 are bounded by latitudes 0°, 30°N and longitudes 0°, 45°

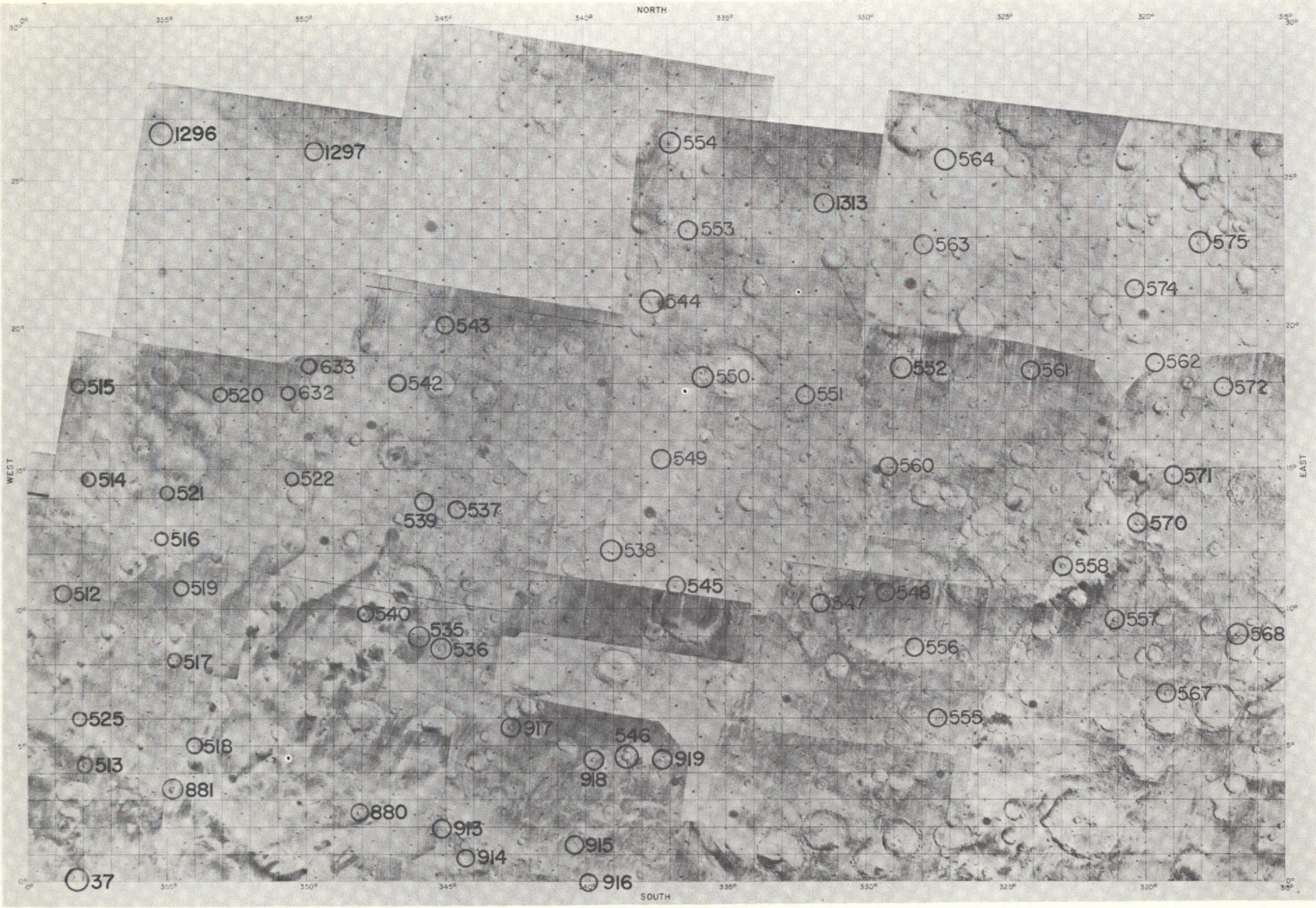

Fig. 14—Control points identified on USGS MC-12 are bounded by latitudes 0°, 30°N and longitudes 315°, 0°

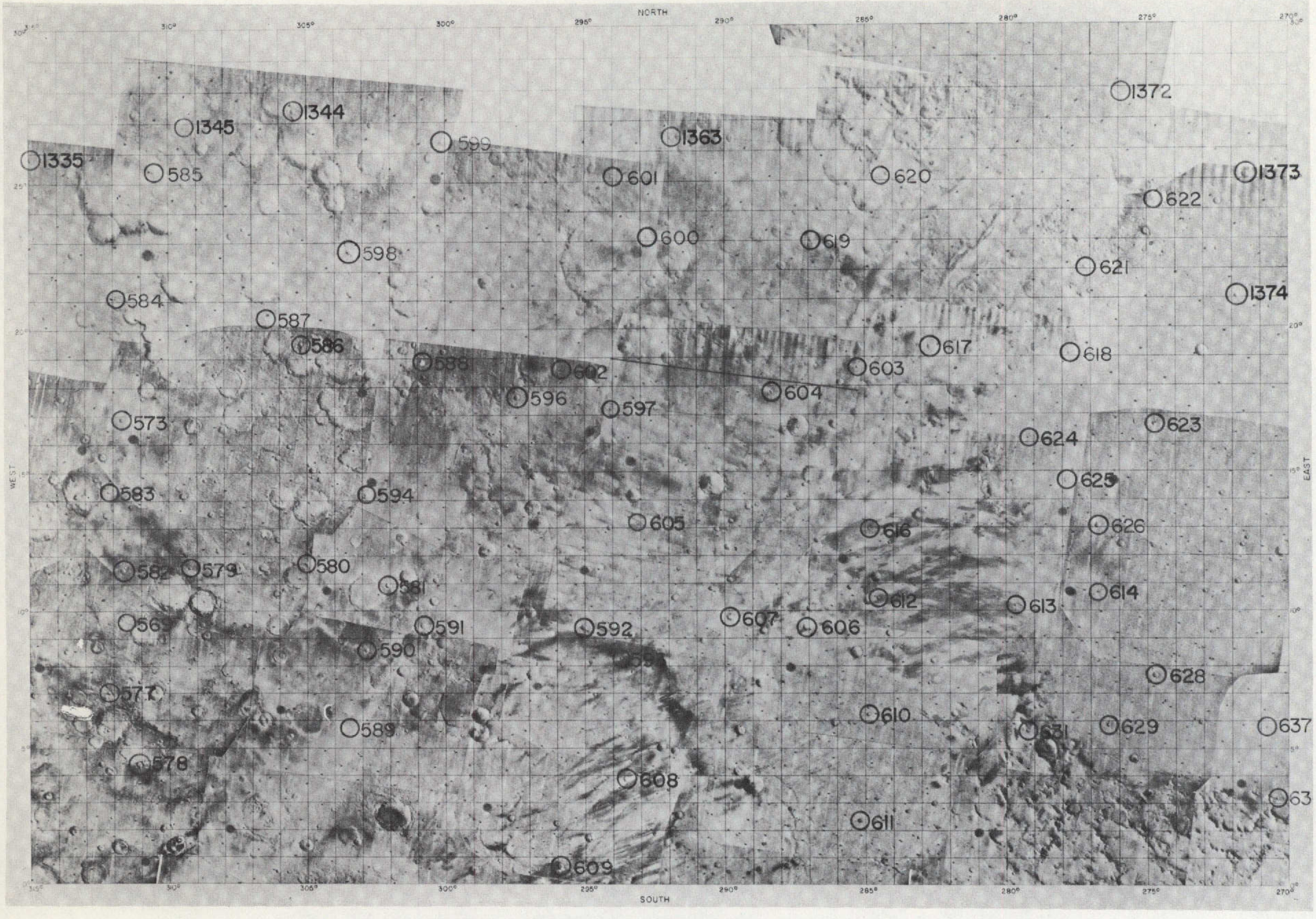

Fig. 15—Control points identified on USGS MC-13 are bounded by latitudes 0°, 30°N and longitudes 270°, 315°

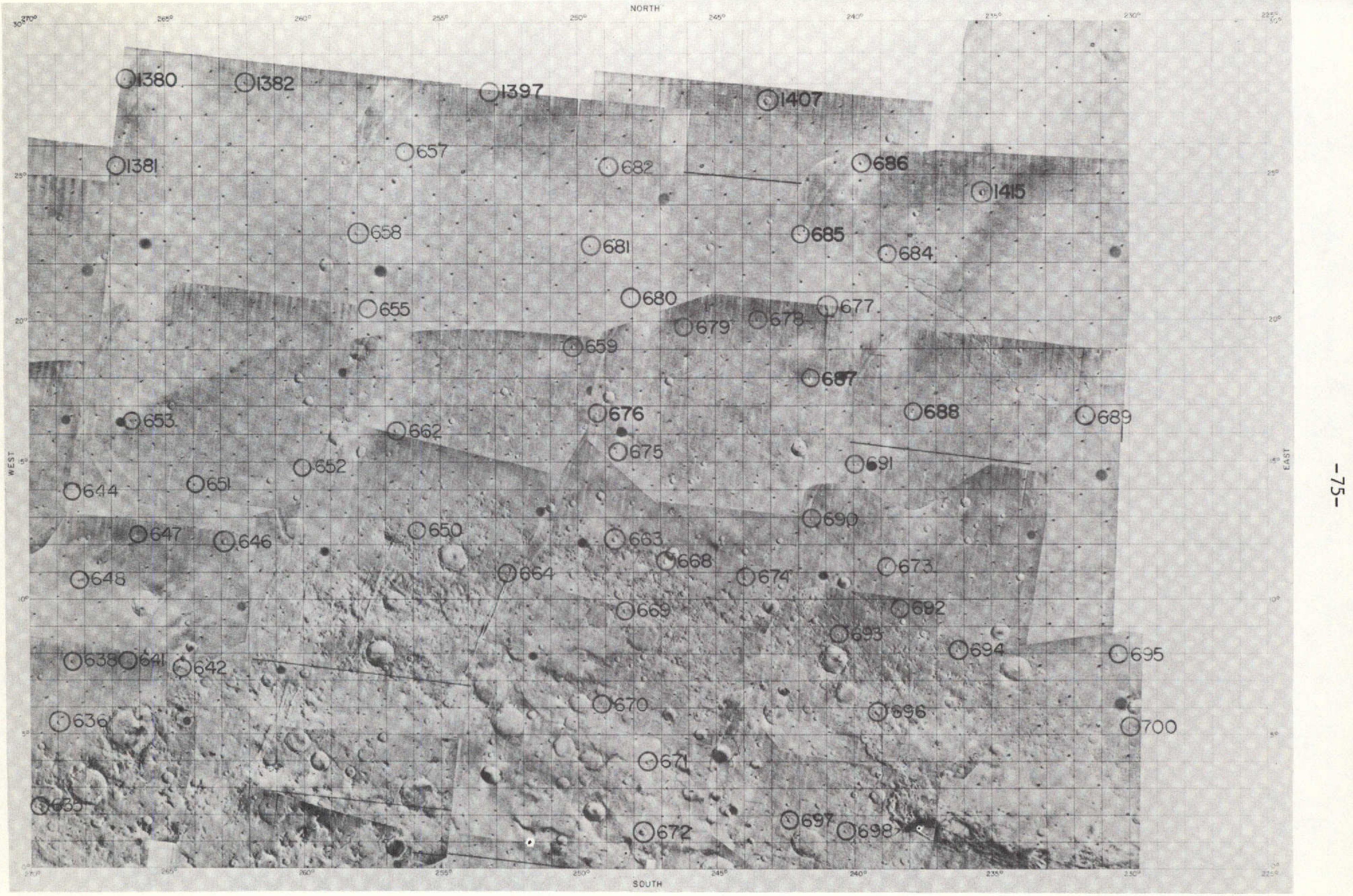

Fig. 16— Control points identified on USGS MC-14 are bounded by latitudes 0°, 30°N and longitudes 225°, 270°

Fig. 17— Control points identified on USGS MC-15 are bounded by latitudes 0°, 30°N and longitudes 180°, 225°

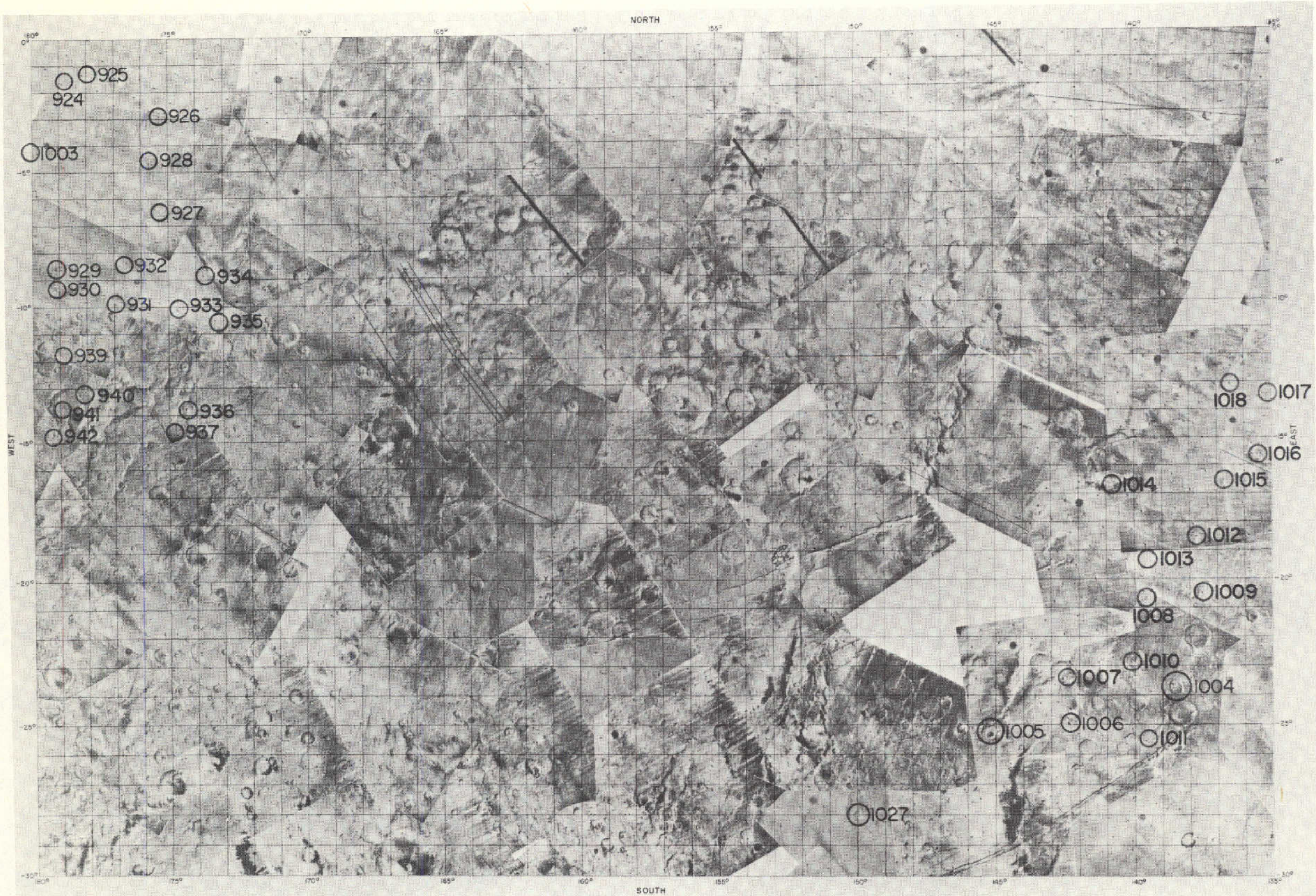

Fig. 18 — Control points identified on USGS MC-16 are bounded by latitudes 0°, 30°S and longitudes 135°, 180°

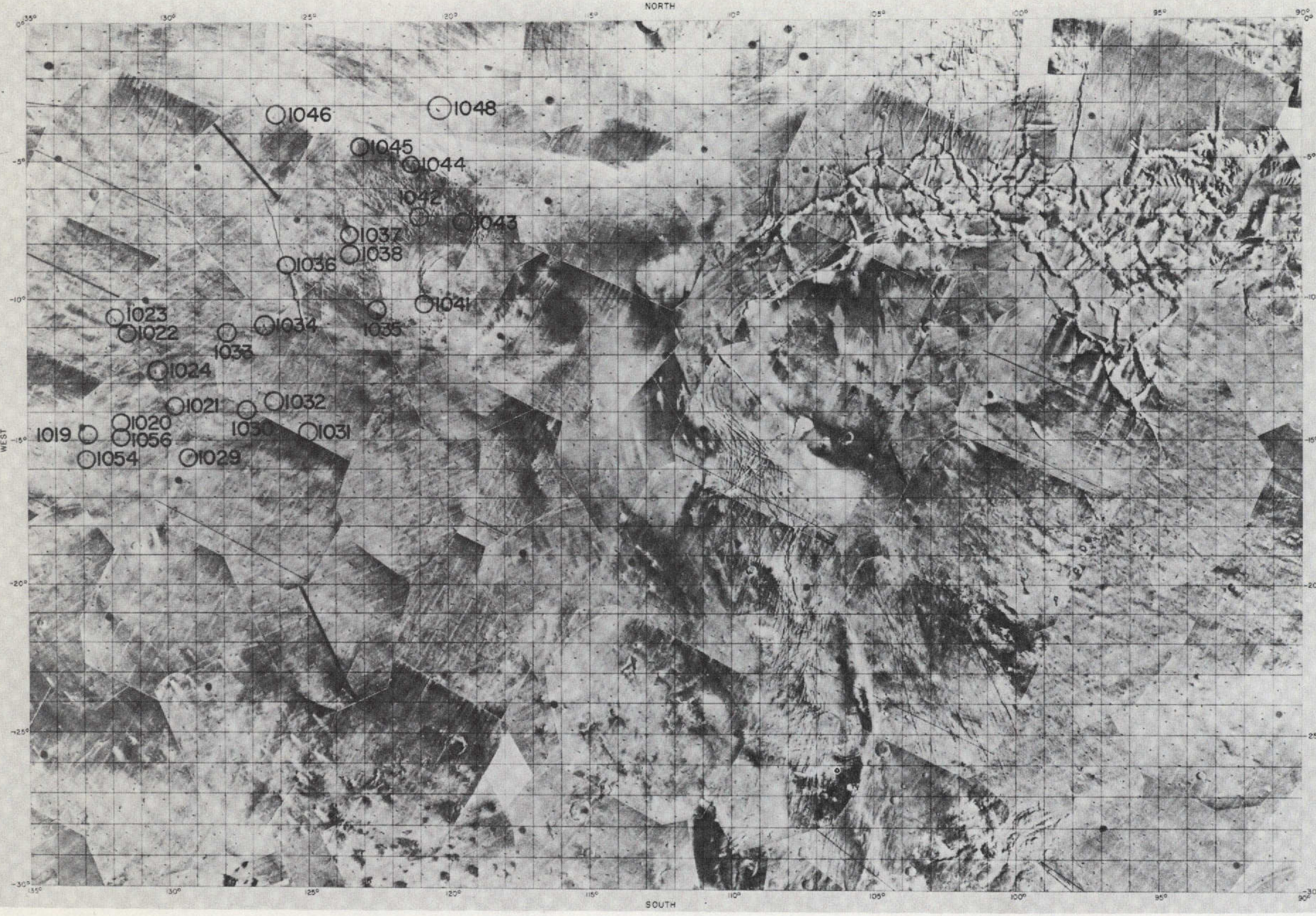

Fig. 19—Control points identified on USGS MC-17 are bounded by latitudes 0°, 30°S and longitudes 90°, 135°

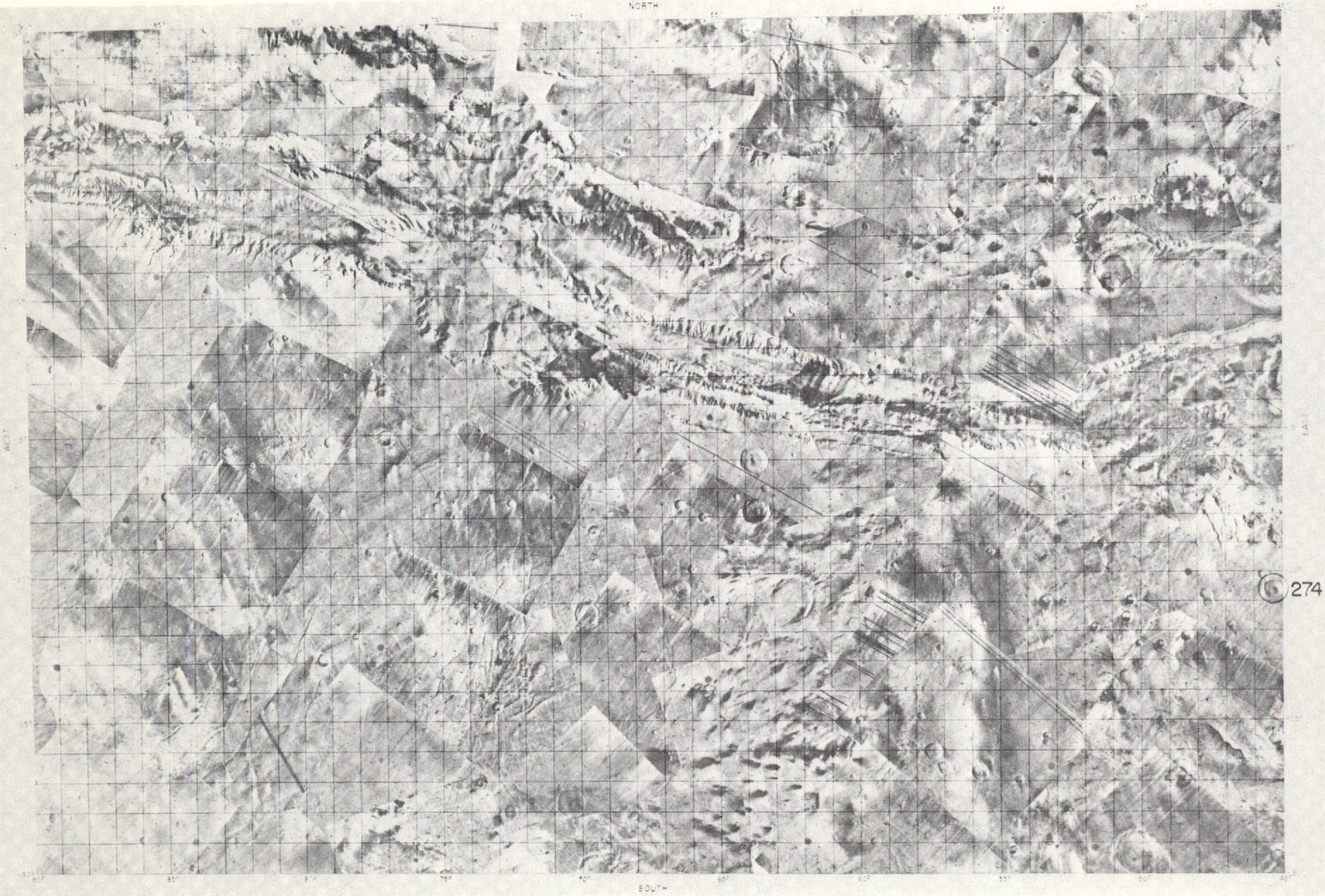

Fig. 20— Control points identified on USGS MC-18 are bounded by latitudes 0°, 30°S and longitudes 45°, 90°

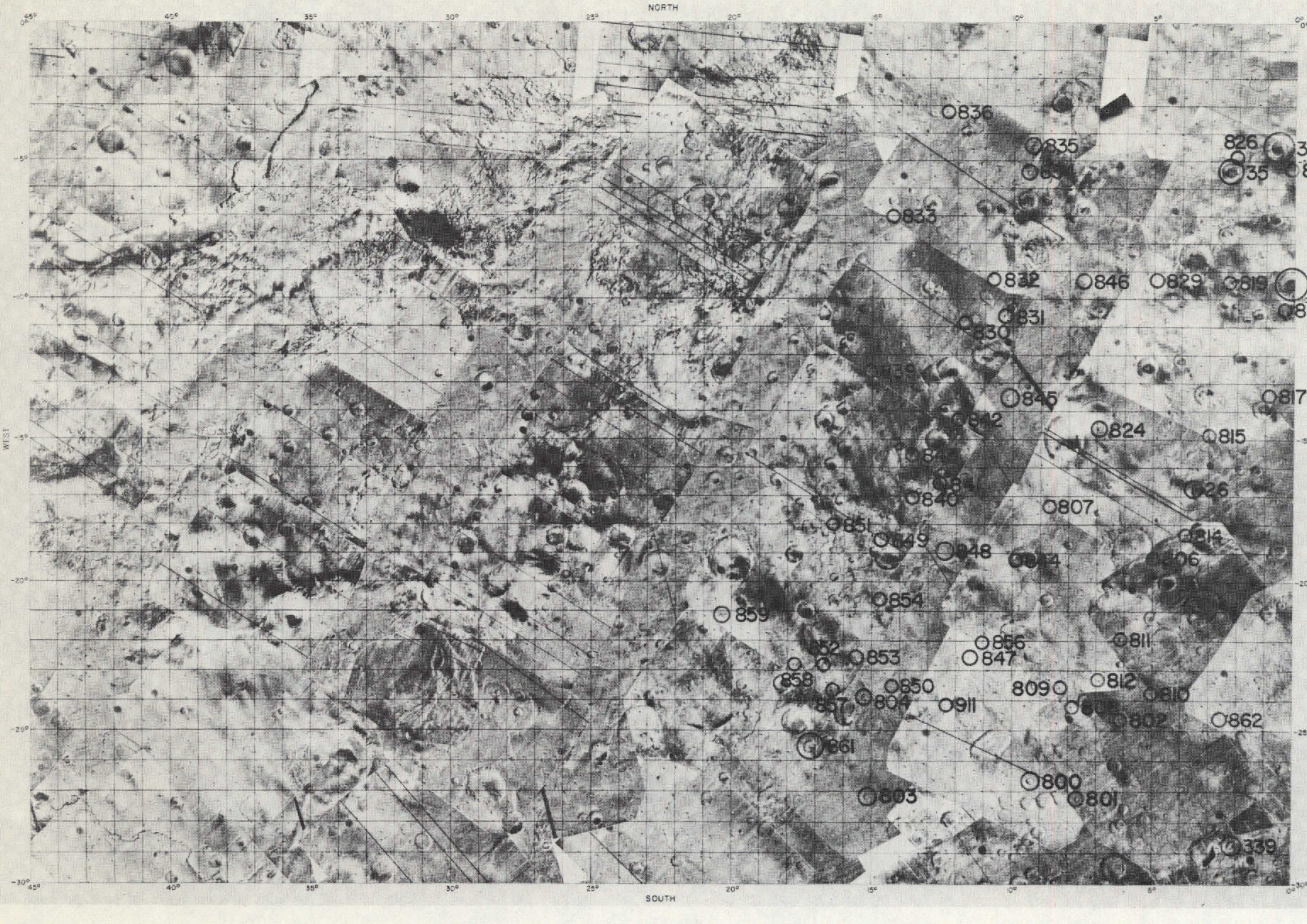

Fig. 21 — Control points identified on USGS MC-19 are bounded by latitudes 0°, 30°S and longitudes 0°, 45°

Fig. 22—Control points identified on USGS MC-20 are bounded by latitudes 0°, 30°S and longitudes 315°, 0°

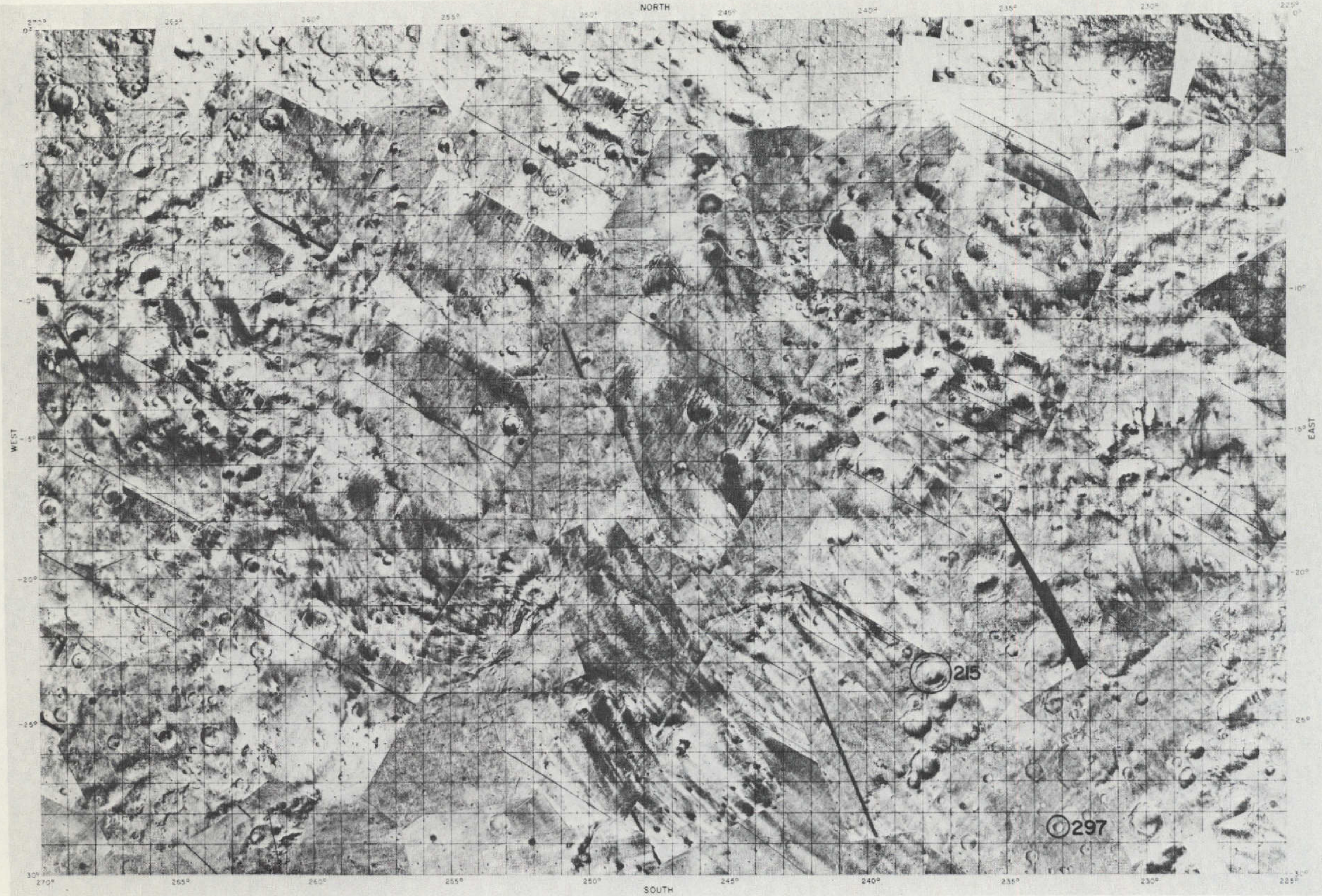

Fig. 23— Control points identified on USGS MC-22 are bounded by latitudes 0°, 30°S and longitudes 225°, 270°

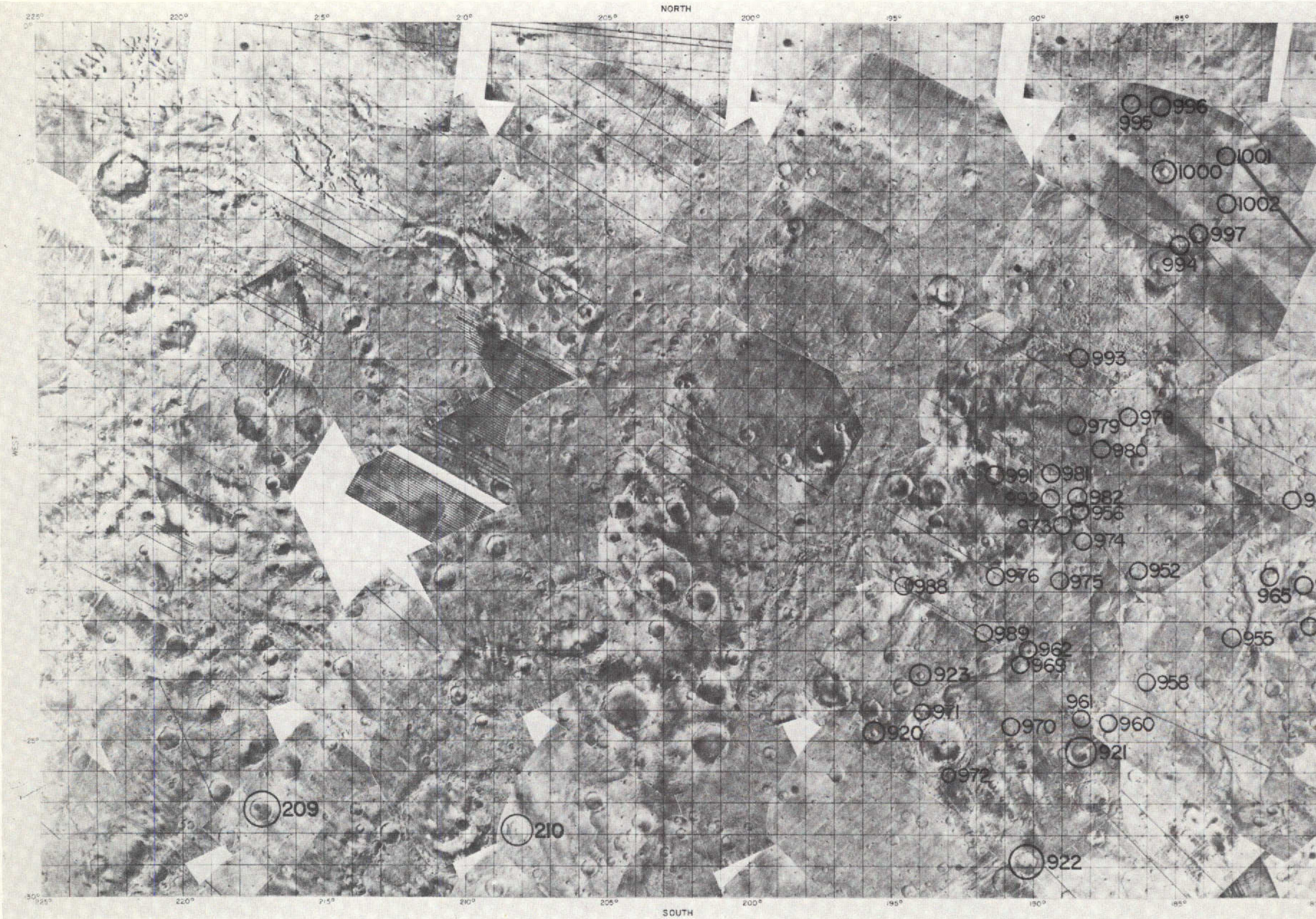

Fig. 24—Control points identified on USGS MC-23 are bounded by latitudes 0°, 30°S and longitudes 180°, 225°

Fig. 25— Control points identified on USGS MC-24 are bounded by latitudes 30°S, 65°S and longitudes 120°, 180°

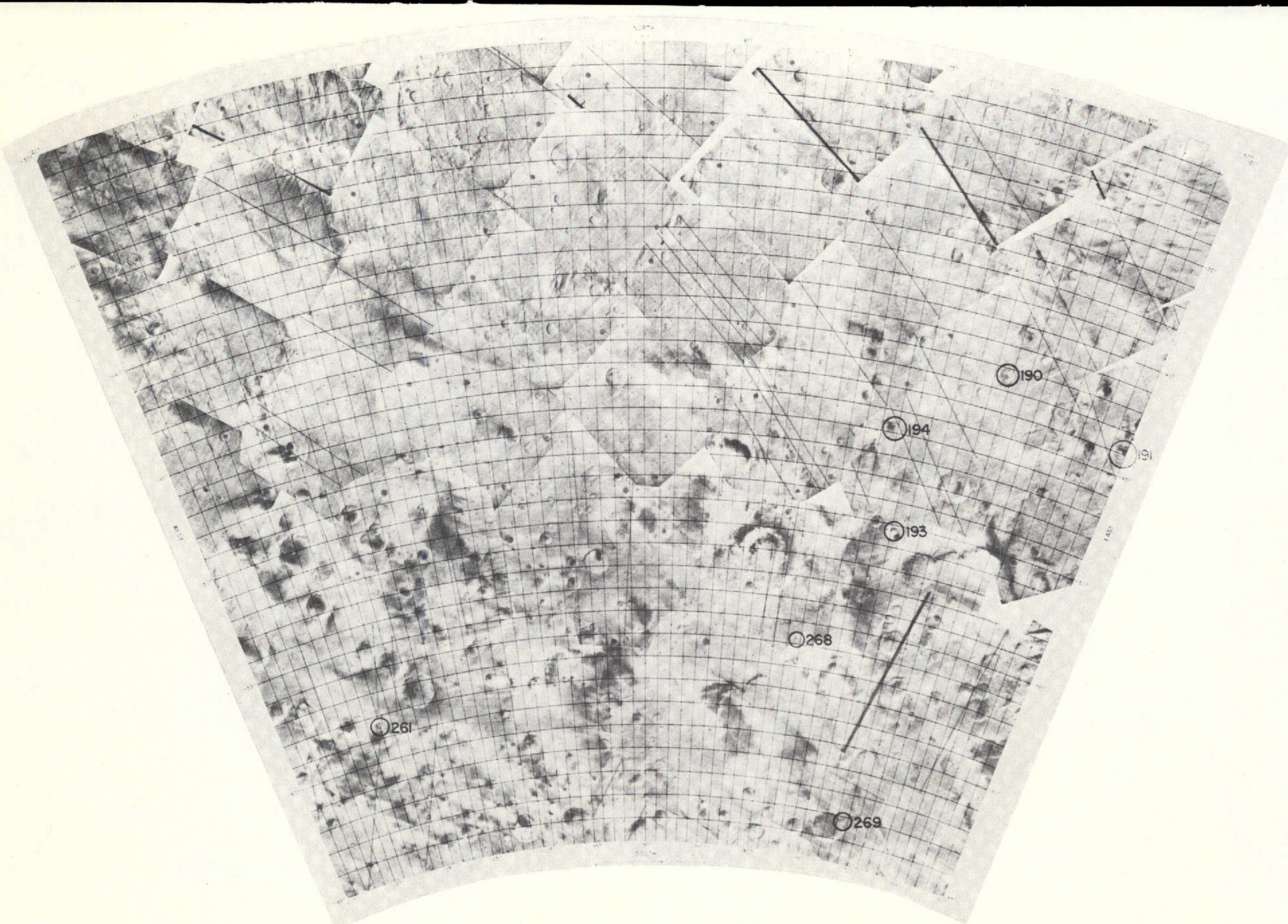

Fig. 26 — Control points identified on USGS MC-25 are bounded by latitudes 30°S, 65°S and longitudes 60°, 120°

Fig. 27— Control points identified on USGS MC-26 are bounded by latitudes 30°S, 65°S and longitudes 0°, 60°

Fig. 28 — Control points identified on USGS MC-27 are bounded by latitudes 30°S, 65°S and longitudes 300°, 0°

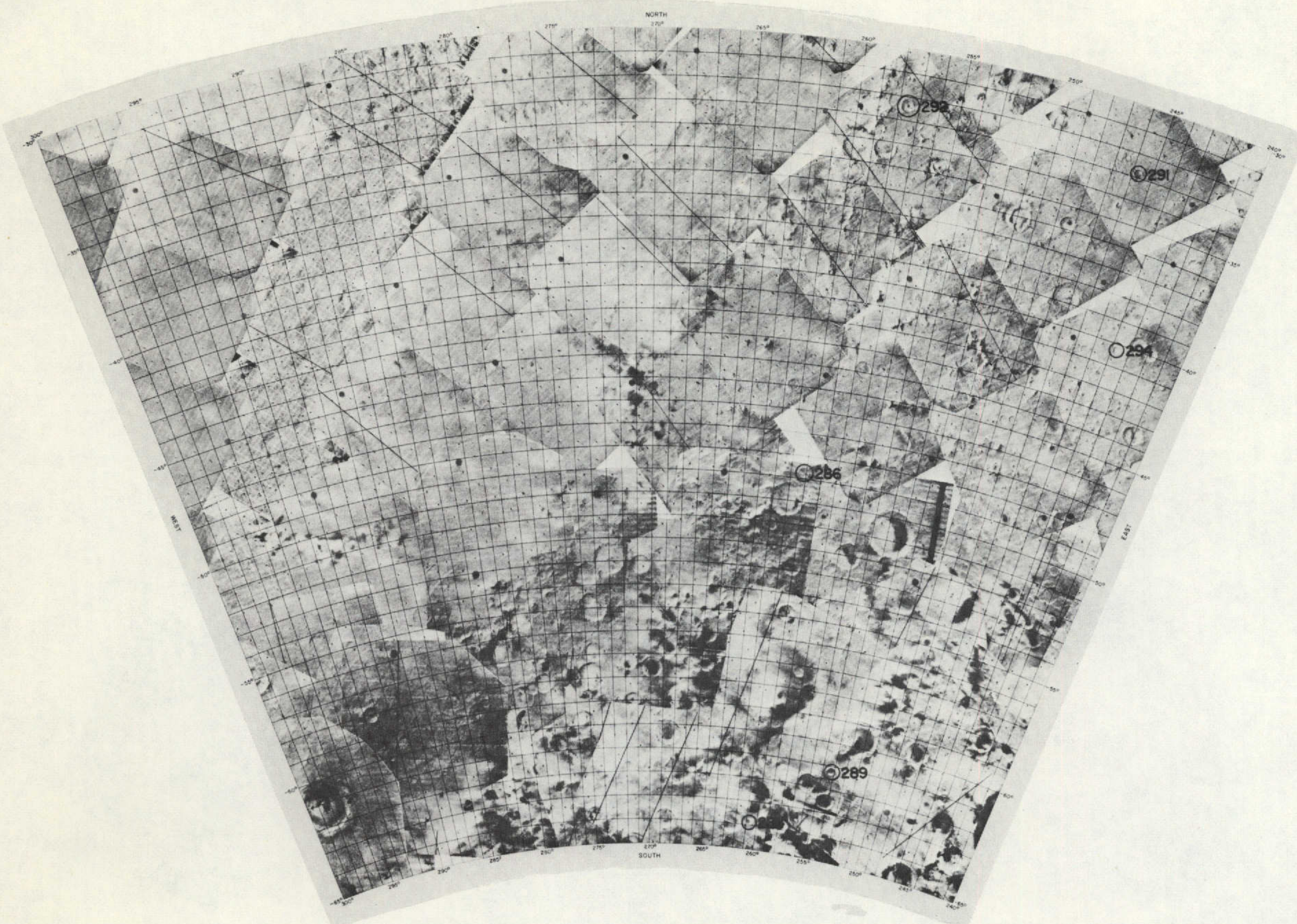

Fig. 29— Control points identified on USGS MC-28 are bounded by latitudes 30° S, 65° S and longitudes 240°, 300°

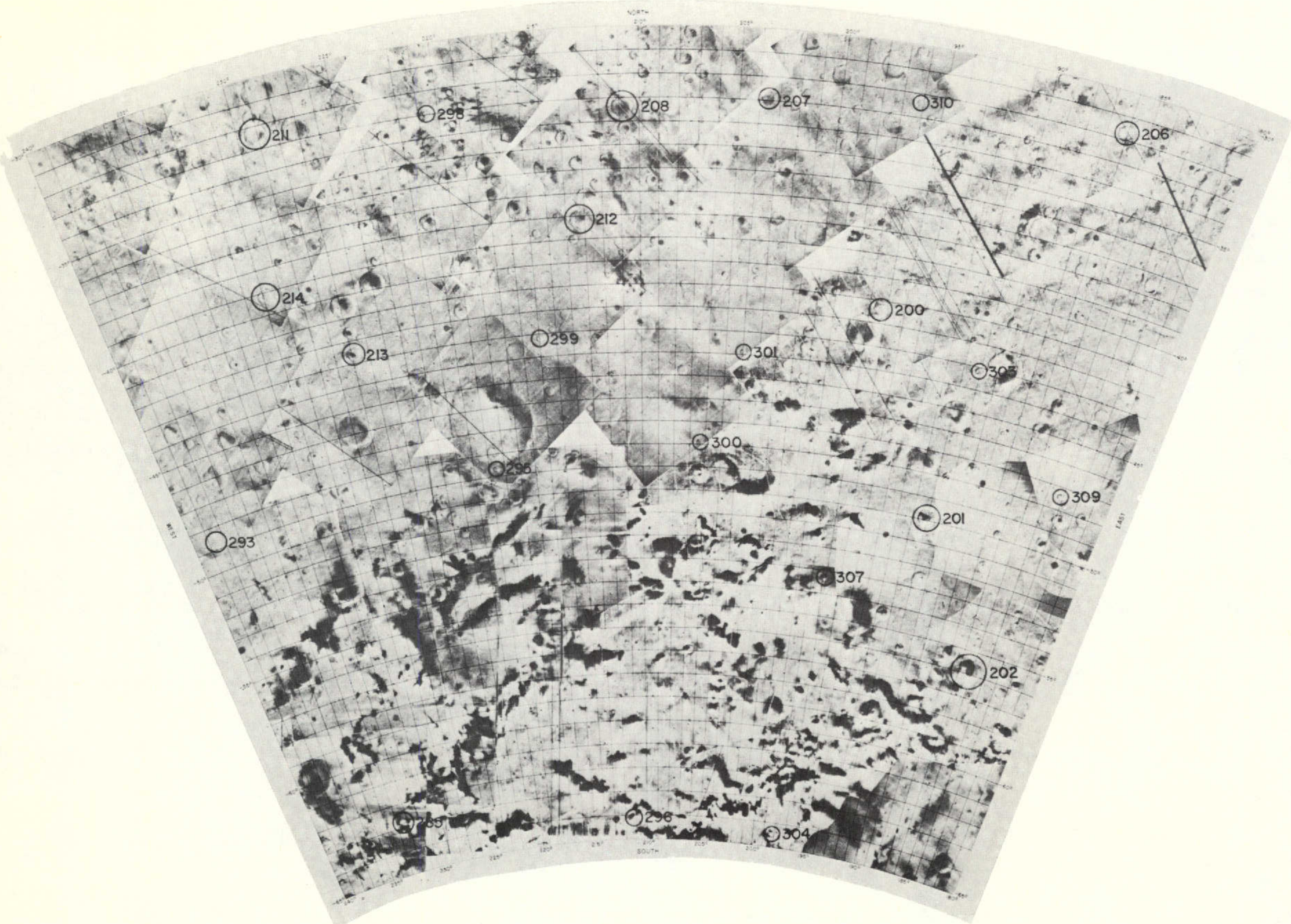

Fig. 30 — Control points identified on USGS MC-29 are bounded by latitudes 30° S, 65° S and longitudes 180°, 240°

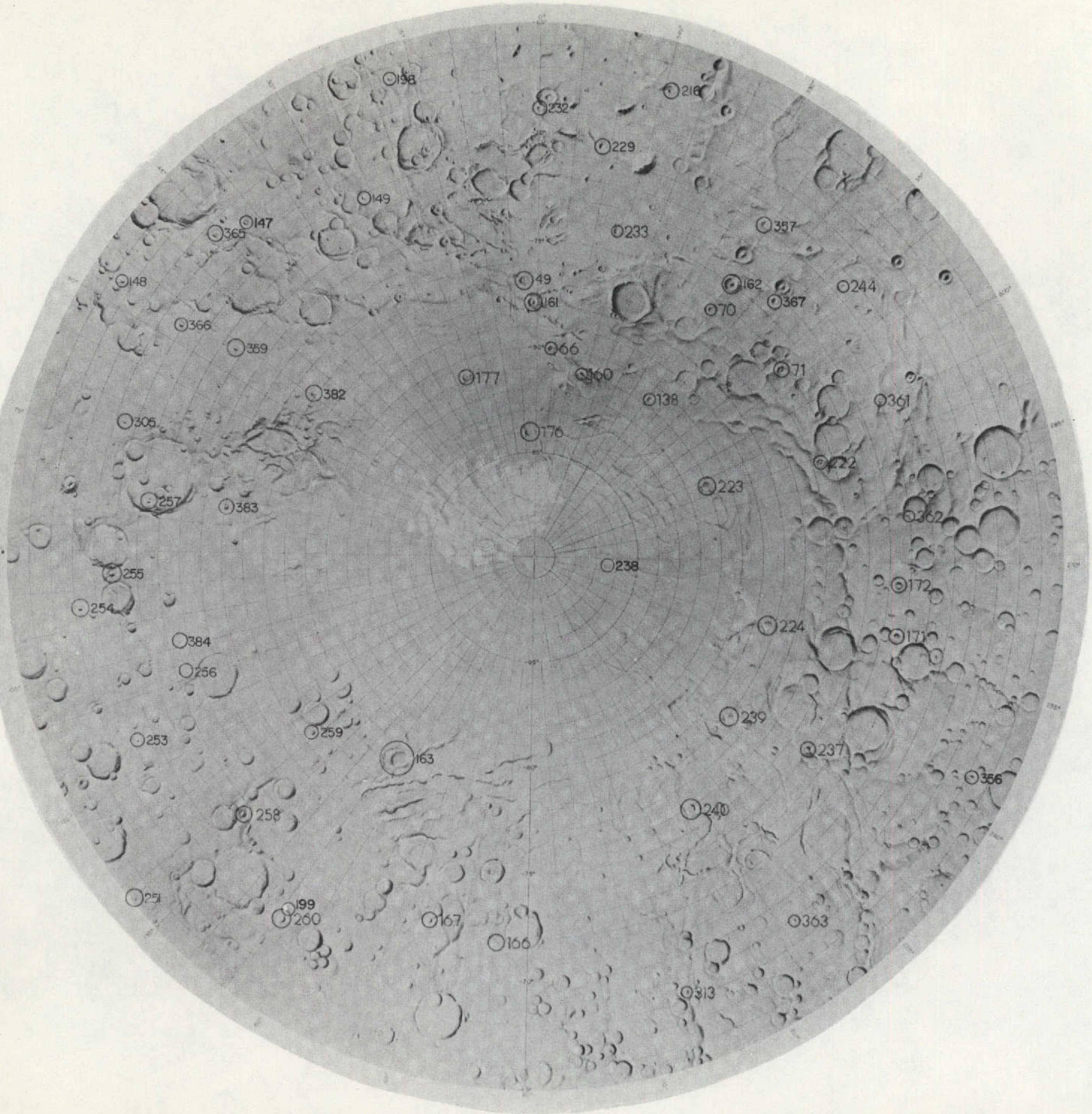

Fig. 31— Control points identified on USGS MC-30 are south of 65° S

REFERENCES

Davies, M. E., Coordinates of Features on the Mariner 6 and 7 Pictures of Mars, *The Rand Corporation, R-896-NASA*, October 1971; *Icarus, 17*, p. 116, 1972.

Davies, M. E., Mariner 9 Control Net of Mars, *The Rand Corporation, R-1122-JPL*, October 1972.

Davies, M. E., and R. M. Berg, A Preliminary Control Net of Mars, *The Rand Corporation, RM-6381-JPL*, November 1970; *J. Geophys. Res., 76*, p. 373, 1971.

de Vaucouleurs, G., Charting the Martian Surface, *Sky and Telescope, 30*, 196, 1965.

de Vaucouleurs, G., Research Directed Toward Development of a Homogeneous Martian Coordinate System, *Final Report, AFCRL-69-0507*, Air Force Cambridge Research Laboratories, 1969.

de Vaucouleurs, G., M. E. Davies, and F. M. Sturms, Jr., Mariner 9 Areographic Coordinate System, *J. Geophys. Res.*, 1973 (forthcoming).

Gillespie, A. R., and M. Soka, "An Orthographic Photomap of the South Pole of Mars from Mariner 7," *Icarus, 16*, 522-527, 1972.

Kliore, A. J., D. L. Cain, G. Fjeldbo, B. L. Seidel, M. J. Sykes, and S. I. Rasool, The Atmosphere of Mars from Mariner 9 Radio Occultation Measurements, *Icarus, 17*, 484, 1972.

Kreznar, J., User and Programmer Guide to the MM'71 Geometric Calibration and Decalibration Programs, Interoffice Memorandum 824-IPL/72-623, Jet Propulsion Laboratory, 1972 (unpublished data).

Rofer, C. A., Map 2 VICAR Program, 124-IPL/72-606, Jet Propulsion Laboratory, 1972 (unpublished data).

Strums, F. M., Jr., Polynomial Expressions for Planetary Equators and Orbit Elements with Respect to the Mean 1950.0 Coordinate System, *JPL 32-1508*, January 1971.